CHALMERS

Operation of HVDC Grids in Parallel with AC Grids

Master of Science Thesis in Electric Power Engineering

GUSTAVO PINARES CCORIMANYA

Department of Energy and Environment
Division of Electric Power Engineering
CHALMERS UNIVERSITY OF TECHNOLOGY
Göteborg, Sweden, 2010

Operation of HVDC Grids in Parallel with AC Grids

GUSTAVO PINARES CCORIMANYA

Examiner: Doctor Tuan A. Le

Supervisor: Professor Math Bollen, STRI AB

Department of Energy and Environment

Division of Electric Power Engineering

CHALMERS UNIVERSITY OF TECHNOLOGY

Göteborg, Sweden 2010

Operation of HVDC grids in Parallel with AC Grids
GUSTAVO PINARES CCORIMANYA

Department of Energy and Environment
Chalmers University of Technology
SE-412 96 Göteborg
Sweden
Telephone + 46 (0)31-772 1000

Master thesis conducted at STRI AB

Chalmers Bibliotek, Reproservice
Göteborg, Sweden 2010

Operation of HVDC Grids in Parallel with AC Grids

GUSTAVO PINARES CCORIMANYA
Department of Energy and Environment
Division of Electric Power Engineering
Chalmers University of Technology

Abstract

In this thesis, the operation of multi-terminal VSC-HVDC grids is investigated. The advantages of an HVDC grid are the possibility of transporting large amount of power over long distances and the possibility of trading energy among different AC systems. Due to the interest in the exploitation of clean energy sources, far away from consumption center, the idea of using an HVDC grid has become popular in the recent years.

The DC voltage of the HVDC system has been identified to be an important parameter analogous to the frequency in AC systems. The variation of DC voltage indicates power unbalance in the DC grid. If the power is sustainably unbalanced, the DC voltage will either increase or decrease. The DC system dynamic, which is very fast, compared with AC system dynamic, demands fast actions; therefore, automatic measures must take place in order to keep the DC system stable.

A control strategy, to balance the power in the HVDC system, has been proposed in this thesis. The control strategy proposes that, under contingencies, there is at least one converter that regulates the DC voltage, or in other words, balances power. In order to test the control strategy, a converter model was implemented with the help of the Dynamic Simulation Language (DSL) of SIMPOW. Also, a frequency regulation scheme that emulates machine governors is proposed and further tested in this thesis.

The operation of an HVDC grid in parallel with AC grids is tested so that issues such as power oscillations and frequency control can be observed together with the DC grid dynamic. Simulation results show that, with the proposed control strategy, the DC grid remains stable after the simulated outages, even when the converter that regulates the DC voltage is lost. Other important result is that as long as the converters are within its limits, power oscillations don't disturb the DC system at all. When one converter reaches its current limit and its respective AC system is undergoing power oscillations, they will be reflected in the DC grid and the perturbation could be transferred to another AC system. Also, a proposed frequency regulation scheme is, finally, tested and results show that it is feasible that two selected converters cooperate, effectively, on regulating the frequency in one AC system.

Keywords: Multi-terminal HVDC, power balance, frequency regulation.

Acknowledgement

First, I'd like to thank STRI AB for supporting this thesis, especially, to Dr. Asoos Rasool for the confidence placed in me even much time before the beginning of this project.

My deep thanks to my supervisor Prof. Math Bollen for his constant support and guidance during the development of this thesis. Despite his full agenda, we could always find moments for interesting discussions about the thesis and many other topics.

I want to express my gratitude to Dr. Tuan, not only for his contribution as the examiner of this thesis, but also as the lecturer of four courses during the master programme. I appreciate very much the endless energy he spends to support his students in the power system courses.

My warm gratitude goes to Francisco, Thinley and Saman, and all the friends I met at Chalmers in these two years of studies. Their friendship made, certainly, the study period very enjoyable.

My parents, Maxi and Julian, certainly, deserve infinite thanks for being my inspiration and an example to follow. It's a cliché, but I must say that what I got in life is because of them. Cintia and Dieguito are not involved in the development of this thesis, but I'd like to mention them for being the strongest reason for missing Peru.

Finally, to close on a high note, my endless gratitude goes to my lovely wife, Karina, for all her unconditional love, support, and understanding during these two years away. Time for great moments together has come now.

Gustavo Pinares Ccorimanya
Gothenburg, Sweden
June, 2010

Contents

Chapter 1

Introduction

1.1 Background

Traditionally, in the electric power sector, three activities can be identified: generation, transmission and distribution. The generation activity mainly consists of converting different energy sources in electrical energy. Transmission activity is devoted to transport that energy from generation centers to distribution centers. Distribution activity consists of distributing the energy to the costumers.

As electrical systems evolved, technologies for transmitting power also evolved. It is well known that electrical systems started with Edison DC generators, so, in the beginning, transmission systems were direct current (DC) systems [1]. Due to the non-available technology, power transmission could only be done at low voltage levels so the main drawback was that power couldn't be transmitted through long distances due to high losses and voltage drops. Due to this, the alternating current (AC) system won the battle and was worldwide adopted to operate power systems, since transformers allowed to raise voltage level so that losses and voltage drops could be limited.

However, the use of AC voltage brought with it other issues like synchronized operation of synchronous machines, and voltage drop due to reactance of transmission lines. As power demand increased, problems became more evident, and power transmission through AC lines was not only limited by thermal limits, but also by other issues like transient stability and voltage stability, which, in practice, means distance.

The need for transmitting power over long distances has been the main challenge for transmission technologies. In [2] it is mentioned that, in the 1940s, the concern of the Swedish State Power Board (later Vattenfall, now split up into Vattenfall and Svenska Kraftnät) for planning a long transmission system in order to transmit power from a hydro power plant, located in the north, to consumption centers, located in the center of the country. The outcome of this request was the novel AC voltage level of 400 kV, the highest voltage level in the world at that time. A few years later, in 1954, the first direct current link, based on mercury-arc valves, was built to connect the island of Gotland with the mainland of Sweden [2]. Later, in 1967, the mercury-arc valves in one of the

converters of the Gotland's HVDC link were replaced by thyristor valves, becoming the first commercial use of thyristor valves for HVDC applications.

We can see then how transmission systems have evolved accordingly with the technology. Nowadays, the issues are, essentially, the same. Heavily loaded transmission systems and generation centers located far away from the consumption centers. Projects like the HVDC transmission system in Itaipú, Brazil, can show the maturity of thyristor-based HVDC technology. It interconnects two asynchronous AC systems (50 Hz and 60 Hz), with a power rating of 6300 MW, ± 600 kV and around a distance of 800 km. In the 1990s, with the development of switching devices like GTOs and IGBTs, voltage source converters (VSC) were conceived, and in 1999, the first VSC HVDC link came commercially in service.

Renewable energy sources, which are located, generally, far away from consumption centers, are now the driving force for the development of new transmission concepts. Challenging projects are the integration of large scale offshore wind farm located far from shore [3], or the integration of solar energy from the Middle East and North Africa. In those projects, it is claimed that DC transmission systems are more, technically and economically, convenient than AC [4]. Even more, power market integration, which means trading of power over long distances, is another driving force for the development of new transmission concepts. The idea of a Trans-European HVDC grid acting as "electricity highways" [5] is mentioned in reports like [3] or [5].

The idea of a DC grid, with DC lines, DC converter stations, which interconnects more than two terminals, is not a recent idea. As will be shown in the following chapter, multi-terminal HVDC grid was a concept developed, even for classical HVDC, but it is the better controllability options that VSC HVDC technology bears, that makes the latter to be the best candidate to become the core of the future DC grids. However, still there are some technical issues before the "dream" comes true.

Among the issues to be solved, one is the control strategies that should be applied when running a multi-terminal HVDC grid. Which converters should regulate the voltage, and which should control the active power are some of the questions to be answered. Also the operation mode under contingencies is an issue with regard to HVDC grid operation.

Another concern is protection of cables (lines) and converters. How to detect a fault, how to coordinate the operation of protective devices, and how to isolate (DC Breakers) the faulted element are questions to be answered in this regard.

Meanwhile, exhaustive research works on HVDC grids feasibility are being carried out and, hopefully, in the near future, a reliable and more efficient solution for new transmission system demands will be met.

1.2 Aims and Scope

The aim of this thesis is to investigate VSC based HVDC grids from the operation point view. In this regard, it has been identified that, in HVDC transmission systems, DC voltage regulation, which can be translated into power balance, can be compared to frequency regulation in AC systems.

From this, the first objective of this thesis is to devise a control strategy in order to ensure that the DC voltage will be regulated (i.e. the power will be balanced) despite the outage of the voltage regulating converters or if these have reached their current limit. A derived task from this is to analyze the DC system dynamic and what impact it would have in the connected AC systems.

A second objective is to investigate the feasibility of frequency regulation between separate AC systems, but DC interconnected.

The term “multi-terminal” HVDC grid is used in the literature and will be used throughout this thesis. The following aspects will be investigated in this thesis:

- Previous research works on multi-terminal HVDC.
- Control Strategies for multi-terminal VSC – HVDC for controlling DC voltage, i.e. balancing power in the DC grid.
- Modeling of VSC – HVDC for electromechanical dynamics in the AC system and DC grid dynamics in the DC system. Models will be developed with the dynamic simulation language (DSL) of SIMPOW.
- Investigation of AC system interaction with DC system through simulations. The feasibility of frequency regulation among non-synchronously interconnected AC grids, but DC interconnected, will be investigated.

Fault analysis and electromagnetic transient simulations are out of the scope of this thesis. The thesis is not intended to develop exhaustive control models. Control models are simple, and, in fact, are used as a tool to analyze, with simulations, the feasibility and the benefits of the proposed control strategies for HVDC operation.

1.3 Outline of the thesis

This thesis is organized as follow:

In Chapter 1, an introduction of the thesis work is presented. The aim and scope of the thesis are stated as well.

Chapter 2 starts with a brief introduction to multi-terminal HVDC. After that, it is devoted to devise a control strategy that ensures the secure operation of the HVDC grid.

Control strategies presented in the literature will be reviewed and discussed. Finally, a proposed control strategy, with the aim of having a secure operation under converter outages is presented.

In Chapter 3 and 4, modeling issues are presented. Chapter 3 introduces the software used for the modeling task and how pre-defined elements are modeled in the used software package. Chapter 4 deals with the controller modeling and, in the end, a brief analysis of the DC dynamic is presented. A Frequency regulation scheme is also introduced.

In Chapter 5, the proposed scheme is simulated in an HVDC grid that connects separate AC systems. Frequency regulation scheme is also analyzed.

Final remarks of the thesis are presented in Chapter 6.

Chapter 2

Operation of Multi-terminal HVDC Grids

In this chapter, first, a brief review of principal aspects of multi-terminal HVDC is presented. Following to this, a review of the literature regarding control strategies for operation of multi-terminal HVDC is presented. It has been found that the DC voltage is an important parameter in the DC grid, comparable to the frequency in the AC grid. The behavior of the DC voltage reflects the balance of power in the DC grid, as will be shown later in this chapter.

The term “input power” will be used to refer the power that is transferred by the converter from the AC grid to the DC grid, and, “output power”, to refer the power that is transferred by the converter from the DC grid to the AC grid.

2.1 Multi-terminal HVDC Overview

Contrarily to what can be thought, power transmission through a multi-terminal HVDC is not a new idea. Around decade after the first commercial HVDC link was put in operation, research work on the idea of multi-terminal HVDC started. Protection, control, and modeling have been covered since the 1960’s [6] for the application of line-commutated converters in multi-terminal HVDC. Next, some issues regarding multi-terminal HVDC are briefly presented.

2.1.1 Configuration

Basically, two configurations are found in the literature [7]: Parallel-connected DC system and series-connected DC systems. Both concepts are shown in the Figure 2-1.

In a parallel-connected DC system, the voltage is control by one converter while the others control current. One of the advantages of this type of configuration is that, if one element is disconnected, the system can still remain in operation. Another advantage is that losses level is lower as compared with series connection [8]. However, one drawback

of parallel configurations is that a perturbation in the DC side will affect the whole system [7]. With classical HVDC, another drawback is that power reversal in one converter will require voltage reversal in the whole system, so mechanical switching is required [7]; however, this drawback is overcome with voltage source converters.

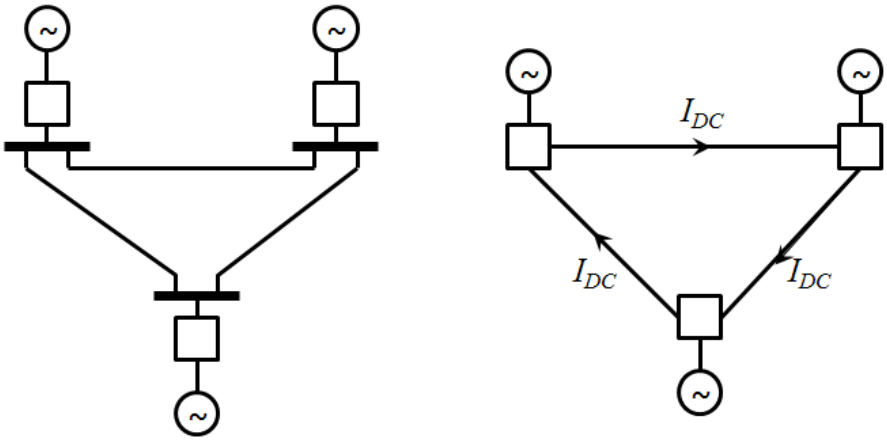

Figure 2-1 Multi-terminal configurations. Right: parallel configuration, left: series configuration

In the series-connected DC system, the current is controlled by one converter and it is the same along the whole circuit. Other converters control the power by varying the DC voltage at its terminals. The main advantage of this configuration is that, for classical HVDC, mechanical switching is not need. On the other hand, one drawback is that this type of configuration bears higher losses [7]; another drawback is that insulation coordination is a more difficult issue [8]. One major disadvantage is that if one part of the DC circuit is disconnected the whole DC system will be lost [9].

In practice, only parallel configuration has been used and considered due to its better flexibility and lower losses [8].

2.1.2 Control

This aspect of multi-terminal HVDC systems will be presented in more detail in Section 2.3. For classical HVDC, mostly, the widely used current margin control is extended to multi-terminal configurations [6], [8]. Other control strategies for classical HVDC are presented also in [6].

For voltage source converters, mainly two control strategies are proposed: voltage margin control and droop control. These control strategies are presented and discussed in Section 2.3

2.1.3 Protection

Protection is, perhaps, one of the major concerns for the operation of multi-terminal HVDC. In point to point configurations, fault in the DC side are cleared disconnecting the whole DC system using the breakers in the AC side. However, in a DC system with more than two terminals, it is desirable that, when a fault in the DC system occurs, only the faulty elements are disconnected and the healthy elements remain in operation.

The main design problems of the DC breakers are that no zero crossing occurs naturally in DC systems, as in AC systems [7]. In [7] also, it is presented a circuit breaker that creates a zero crossing current through a resonant circuit.

Fault detection is a more challenging topic, and [7], for classical HVDC, and [10], for VSC, can be reviewed for more details. Fault detection is important to achieve selective disconnection of faulted elements in the DC system. Circuit breakers can be located as shown in Figure 2-2 in order to ensure selective disconnection.

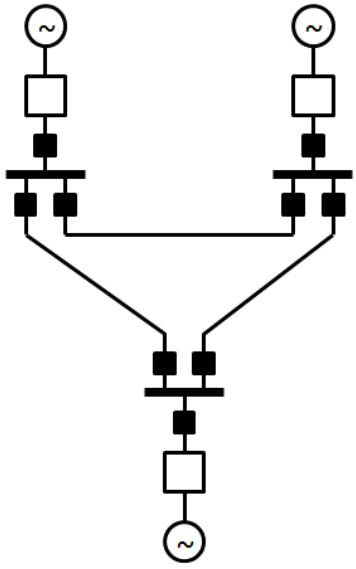

Figure 2-2 DC breaker locations to selective disconnect faults in the DC grid.

2.1.4 Example of projects around the world

In [11] three projects are mentioned as examples of multi-terminal HVDC system currently in operation. They are the following:

Sardinia-Corsica-Italy (SACOI) System Tapping

Sardinia and Italy were interconnected through a monopolar classical HVDC link since 1967. The rated power of this link was 200 MW and the rated voltage 200 kV. An additional terminal was added at Corsica in 1986 [12] with a rated power of 50 MW.

The Hydro Quebec – New England Five Terminal 450 kV DC System

Commissioned between 1986 and 1992, in Canada, initially, the original idea was to build a five link radial multi-terminal HVDC. The rated voltage was selected to be ± 450 kV and rated power of 2000 MW. After a reassessing of the project, the contractors decided to suspend the commercial integration of two converters [13].

Shin-Shanano Substation

In [14], it is presented a control strategy, which is implemented in an experimental three-terminal back to back DC system. The rated voltage is ± 10.5 kV and 53 MVA for each converter.

2.2 VSC versus Classical HVDC

In this project, the use of VSC technology is assumed for implementation of multi-terminal HVDC. VSC technology has shown to be a promising technology in the future HVDC projects because [15]:

- Active a reactive power can be controlled independently. Classical HVDC requires reactive power from the AC system so compensation is needed.

- Power reversal is accomplished without the need of DC voltage reversal. In a classical HVDC system, in order to reverse the power transmitted, the DC voltage must be reversed.

- The risk of commutation failure is reduced, since VSC uses self-commutated switches, different from the line-commutated switches used by classical HVDC, which need the presence of an AC voltage to commutate.

- Communication is not needed, since controller of rectifiers and inverters operate independently, without the need of information of the remote ends.

- Black start capability is possible with VSC, since the AC voltage is generated from the DC side through a suitable modulation technique. Classical HVDC needs the presence of AC voltage in order to start transmitting power.

- There is no minimum DC power flow restriction, as in the case of classical HVDC, that should be above certain level in order to commutate.

- VSC characteristics make them suitable for multi-terminal HVDC grids. As will be seen in the next Chapters, independent control for each terminal can be developed.

However, VSC technology still has drawbacks to overcome like its limited power transmission capacity and the higher switching losses as compared with classical HVDC.

2.3 Operation Objectives

In [16] it is said that the principle of system operation, in AC systems, is to ensure generation and load balance. The power balancing task in an AC system is complex due to the unpredictable behavior of load, so forecasting is needed in order to help the generation to meet the demand. DC system power balancing task may seem easy since output power and input power are decided by the system operator and fixed in the converters. However complexity comes when contingencies occur, especially when converters in charge of controlling the DC voltage, i.e. balancing power, are suddenly disconnected. Due to of the small amount of energy present in capacitors in the DC grid, fast actions are required in order to keep the DC system stable.

An appropriate operation strategy should ensure the security of the DC system operation. We could take as reference the AC systems, where according to the discussion above, the primary objective is:

- System frequency must be within acceptable limits (i.e. generation and demand balanced).

And a group of “secondary” objectives in order to avoid damages in the system elements are:

- Voltage must be within acceptable limits.
- Generator’s output power (current) must be within the limits.
- Power flow (current) over lines and transformers must be within the limits (thermal limit, transient stability, voltage drop)

In an AC system, these requirements must also be fulfilled for all N-1 contingencies.

Analogously, for a DC grid, the primary objective is:

- DC Voltage within acceptable limits (i.e. input and output power balanced). In this case, high voltages above limits would be harmful for system insulation and low voltages would limit the power transfer.

And the following could be stated as objectives for safe operation:

- Converter currents within their limits.
- Line currents (cables) within the limits.

Similar to AC, these requirements must be fulfilled for all N-1 contingencies. Any control strategy must fulfill all the requirements previously mentioned.

2.4 Control Strategies Proposed in the Literature.

Since this thesis is focused on defining control strategies for multi-terminal HVDC grids, it is helpful to analyze the largely available literature devoted to develop control principles. A great number of publications have been found for classical HVDC, and, to a smaller extent, for VSC HVDC. A brief review of them could be helpful to develop a general control strategy.

Next, some remarkable works are summarized and important concepts are highlighted.

2.4.1 Multi-terminal Grids with Classical HVDC Converters

A number of papers published during the 1960's have investigated different aspects of multi-terminal HVDC grids. Regarding control, the main concern is the power flow balance, which, in other words, means that at least there must be one converter which controls the DC voltage, while the others control power. The converters that regulate the DC voltage at their terminal are like slack buses that balance the power flow in the DC grid.

In [6] a 17-years survey (from 1958 to 1979) is presented, where different aspects, like configuration (series, parallel, radial, meshed), DC line faults, and, the interest of this thesis, converter control were included. For instance, in Figure 2-3 it is shown a set of voltage – current characteristics for three converters corresponding to one of the four control strategies presented in [6]. As can be seen, inverter 2 is operating in voltage control mode, while inverter 1 and the rectifier are both operating in constant current mode.

Another interesting work is [17] where a control based on droop control is presented for classical HVDC. There, the losses in the DC system are neglected. In this type of system, voltage drop doesn't exist so there is a common DC voltage for every terminal. A useful analogy with primary control in AC system is made. The common DC voltage is taken as a signal that reflects the power balance, like frequency in the AC system case.

In this case, voltage droop is used in a similar way as the frequency droop characteristic of primary control. When one rectifier reaches the current limit, the control enters to a constant current mode, making the other rectifiers to balance the power according to their droop characteristic. If there is not enough power to supply the load, the DC voltage will

decrease due to the unbalance between input and output power. Similarly to under-frequency load shedding scheme, the decrease of DC voltage can be used as a signal to reduce the inverter's power setpoints. A simple droop control is proposed in [17], as shown in Figure 2-4.

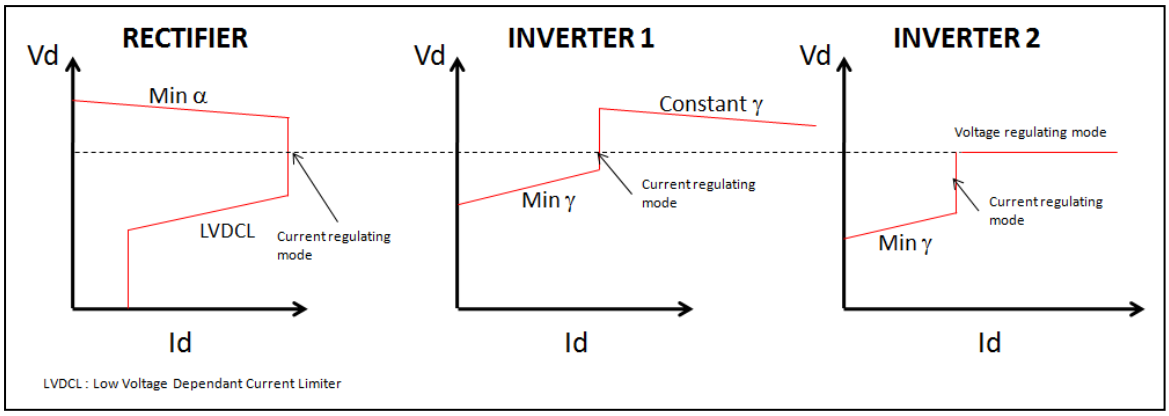

Figure 2-3 Control type A presented in [6].

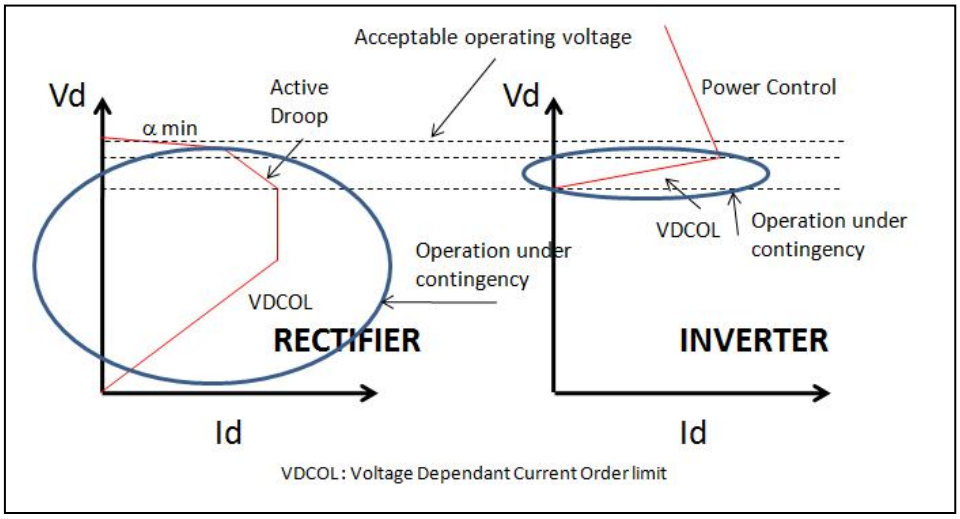

Figure 2-4 Control Characteristics presented in [17]

2.4.2 Multi-terminal Grids with VSC-HVDC Converters

Compared to the classical HVDC technology, where there is plenty of information regarding multi-terminal HVDC, there is little work for the young brother VSC HVDC. It can be identified, after reviewing the literature, that the main driving force for the investigation of multi-terminal VSC-Based HVDC is the integration of large scale offshore wind farms to onshore power systems. For instance, the aim of [11], [18], [19], and [20] is to find strategies to operate a multi-terminal HVDC grid that integrates offshore wind farms and/or offshore oil-platforms to the main onshore grid.

In [18], a three-terminal DC system is analyzed. A brief description of the inner and outer controller is presented, but more important, the voltage margin method is stated [14]. There, operating characteristics, as shown in Figure 2-5, are proposed.

While it is true that in steady state P_a is equal to P_b, this is not the case during transient phenomena, especially when input and output powers are not balanced. For instance, according to [17], if there is a change in P_b (in the positive direction) so that it's higher than the converter limit, then P_a coming from the converter will be all the time lower than P_b. As a consequence, P_a will increase until it reaches the converter current limit, and the difference of power will have to come from the energy stored in the capacitor, which means that the voltage will decrease. Vice versa, if there is a change in P_b (in the negative direction) so that it's higher than the converter limits, there will be an excess of power that will go to the capacitor so the DC voltage will increase.

As stated in [17], when system voltage is lower than the voltage reference, the controller will increase the input power, i.e. P_a, until P_a reaches its upper limit, which instead of being a limit, could be a scheduled power. On the other hand, if the system voltage is higher than the reference voltage, P_a will decrease until it reaches its "scheduled" value. In this case, if terminal A is turned on first, it will set the voltage and supply no power. When terminal B is turned on, the system voltage will be higher than its voltage reference so the power in converter B will be decreased until it reaches the system voltage. The operating point will be as indicated in Figure 2-5.

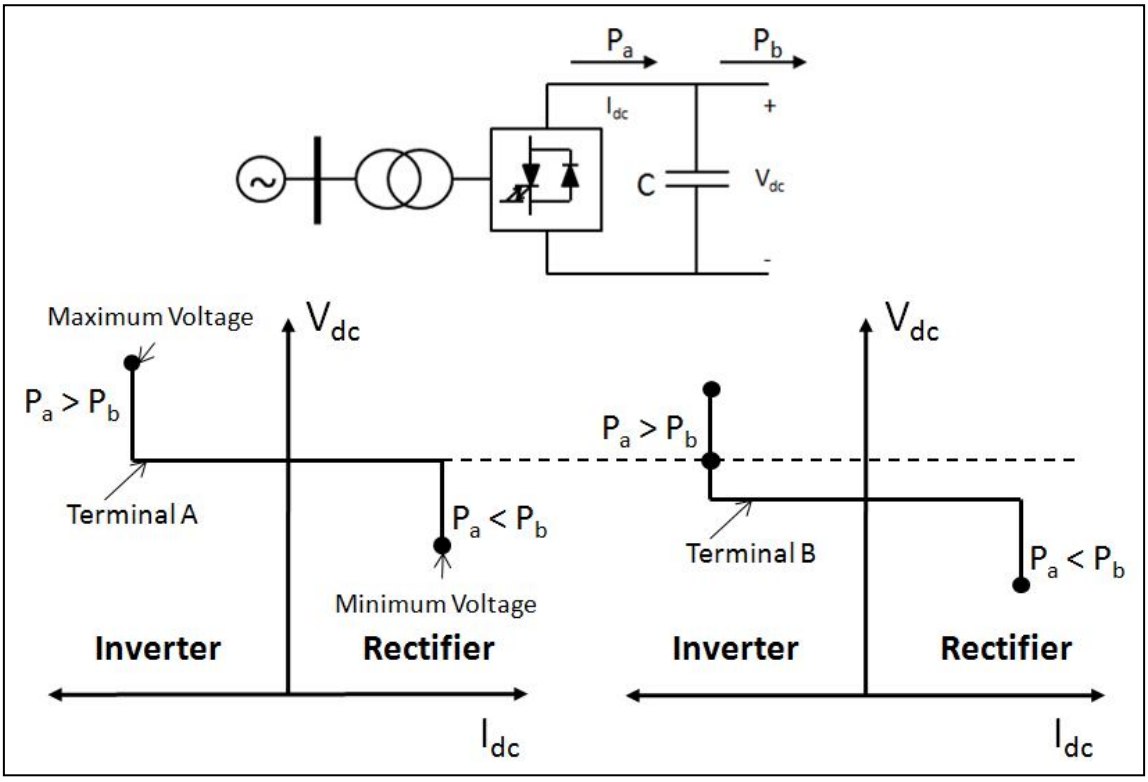

Figure 2-5 Voltage Margin Control proposed in [14]

That procedure was further extended to a multi-terminal system, and operating curves were defined as presented in Figure 2-6. In that case, the operating point for normal operation was shown, and, after the outage of the voltage regulating terminal, the new operating point is shown in Figure 2-6.

In [18], this control method was applied to control the power exchange in a three terminal system. The terminals were a wind farm, an oil platform, and an onshore power system. In this case, the main objective was to supply a constant power to the oil platform station, and it was assumed that the wind farm terminal was the one which sets the voltage.

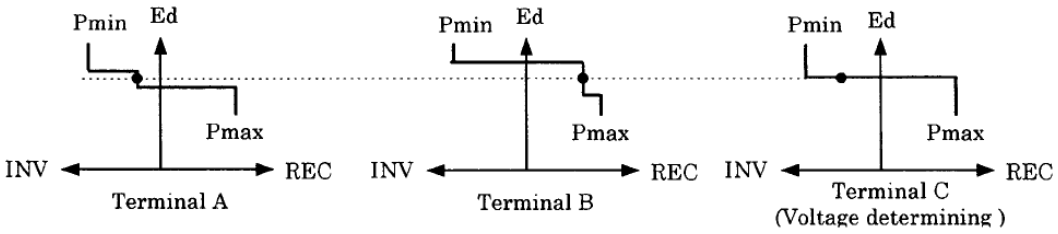

Fig 8. An example of Ed - P characteristics of each terminal

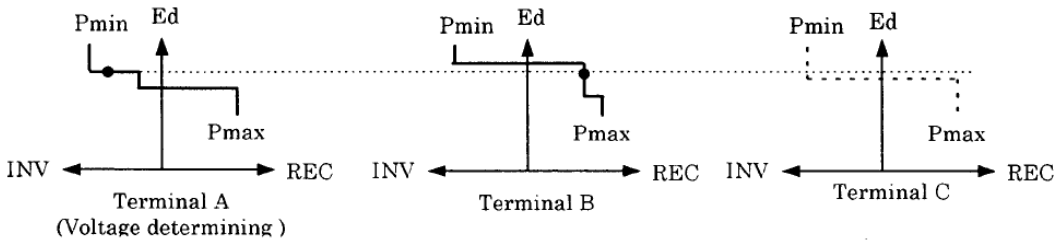

Figure 2-6 Voltage Margin Control proposed in [18] extended to a three-terminal HVDC grid.

In [19], an improvement to the margin voltage control is developed. It is stated that, while it is true that margin voltage control, certainly, manages to designate a voltage control terminal, it is its weakness too. Having only one converter with the hard task of balancing all the input and output powers makes more likely that the new voltage regulating converter reaches its limits and again, a new voltage regulating converter should be designated. In addition, it is claimed in this work that transition from one voltage to another is abrupt so this might result in stressing the DC system.

A four-terminal system is used in [19] to test the proposed control. In Figure 2-7 it is shown the voltage – power characteristic of the controllers. Again, wind farms are set as a voltage regulating converters. Another interesting thing from Figure 2-7 is to see a slope for low voltages in the oil platform load. This droop characteristic is useful when there is deficit of input power, since voltage will decrease in such a way that when reaching this part of the load characteristic, load consumption of the oil platform is decreased, acting like an under-frequency load shedding scheme of AC systems.

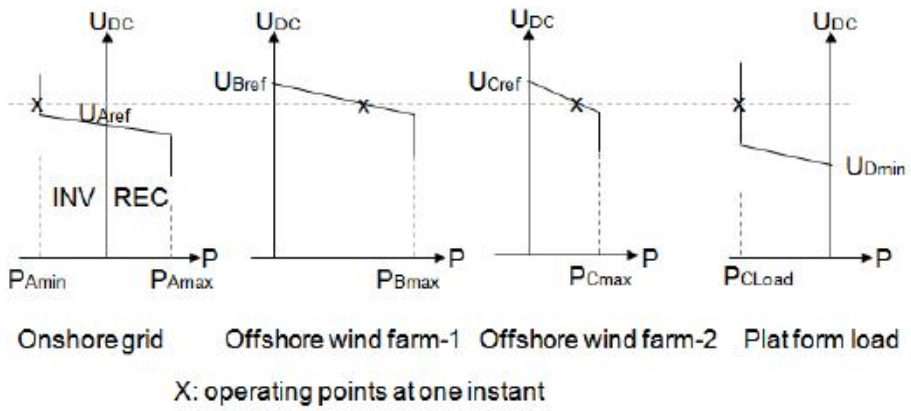

Figure 2-7 Voltage Droop Control proposed in [19] extended to a four-terminal HVDC grid.

2.5 Proposed Control Strategies

Some interesting control strategies have been reviewed; [18] ensures that at least there will be one and only one converter which will be in charge of regulating dc voltage (so it will balance the power flow), [19] presents an improvement so that, under contingencies, there will be the possibility of having more than one converter that will assume the loss of power. Those two works analyze a radial system rather than meshed system with the objective of ensuring power delivery to an oil platform station. A more general approach could be developed if the aim is to work with different AC systems interconnected through a DC grid, or an overlying DC grid that is connected to different locations in an AC system.

A general case of power system operation will introduce general considerations, and the operation objectives should be the same as stated in Section 2.3. A general case might look like the Figure 2-8. There, a number of converters are connected to a meshed DC grid. When having such a system the following questions arise:

- How many converters should control the DC voltage and how should they share the balancing task?
- What should be the location of the voltage regulating converters?
- After a contingency, if voltage-regulating converters reach their limits, how to allocate the balancing task to the other converters?
- In case of deficit of input power, how should inverters behave?
- How to limit the current over a dc line?

Based on these questions, control strategies are defined and presented in the next sections.

2.5.1 Voltage Regulating Converter

The proposed operating characteristic is as shown in Figure 2-9. This simple curve indicates that the converter will set the voltage as long as the output current is within its

limits. It is impossible that two converters connected at the same terminal can have this type of control. However, due to line/cable resistances, it could be possible to have more than one voltage regulating converter at different locations in the DC grid.

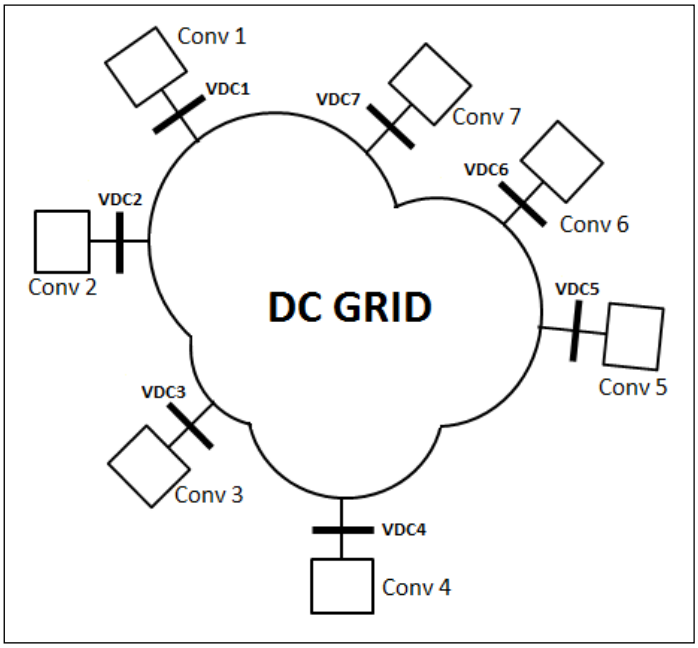

Figure 2-8 Representation of a DC grid.

The task of DC voltage regulating converters is not simply to regulate voltage at its terminal, but, even more important to balance the power in the DC grid. Due to that, the selected converter should have a considerable capacity. Hence, the respective AC system needs to be strong enough to withstand large power variations.

If more than one converter is selected to regulate the DC voltage, the power sharing could be controlled adding a droop characteristic as shown in Figure 2-9. The slope will determine how much the converter contribute to the power balancing task

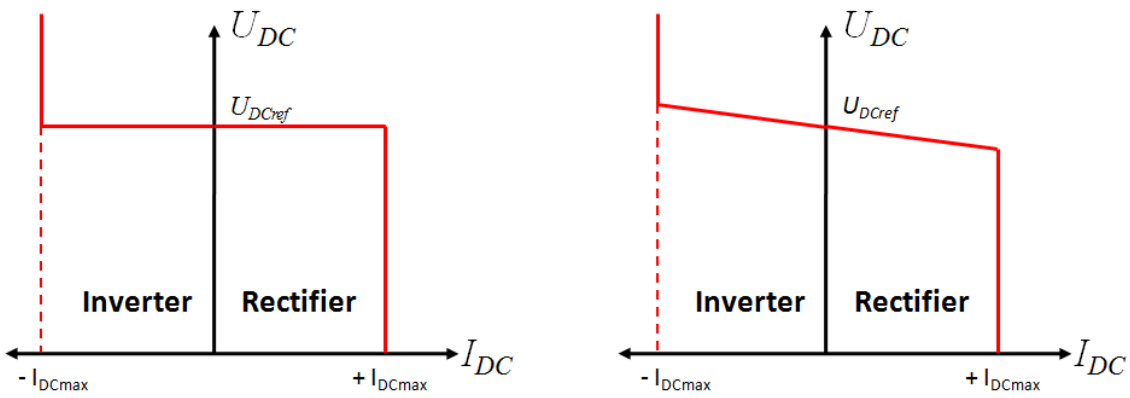

Figure 2-9 Operating characteristic of a voltage regulating converter

2.5.2 Current Regulating Rectifier/Inverter

The proposed characteristic for the current regulating rectifier and inverter is presented in Figure 2-10. There, I_{ref} is the scheduled current, which will be fixed as along as system DC voltage is within U_{DCmax} and U_{DCmin} (Current control mode). If the system's DC voltage goes below U_{DCmin} (Undervoltage control mode), it means that the total input power is lower than the total output power. Therefore, according to the curve, the converter, which is in rectifier mode, will increase its current. On the other hand, if voltage is above U_{DCmax} (Overvoltage control mode), it means that total input power is greater than total output power, so the converter, in rectifier mode, decreases its current to match the total output power, and it could even turn into inverter mode.

If a stiff current control is desired, U_{DCmax} and U_{DCmin} very high and low, respectively, can be selected in such a way that a constant current control is obtained. As mentioned in Section 2.3.1, the strength of the AC system should be evaluated in order to define the operating characteristic. Fixed current could be adopted for weak systems since events in the DC grid would have only limited impact on the conditions in the respective AC systems. As in voltage regulating converters, the slope of the under/over voltage control mode defines the power contribution of each converter to the DC voltage regulating task.

In a similar fashion, a current regulated inverter can be obtained if I_{ref} is selected negative.

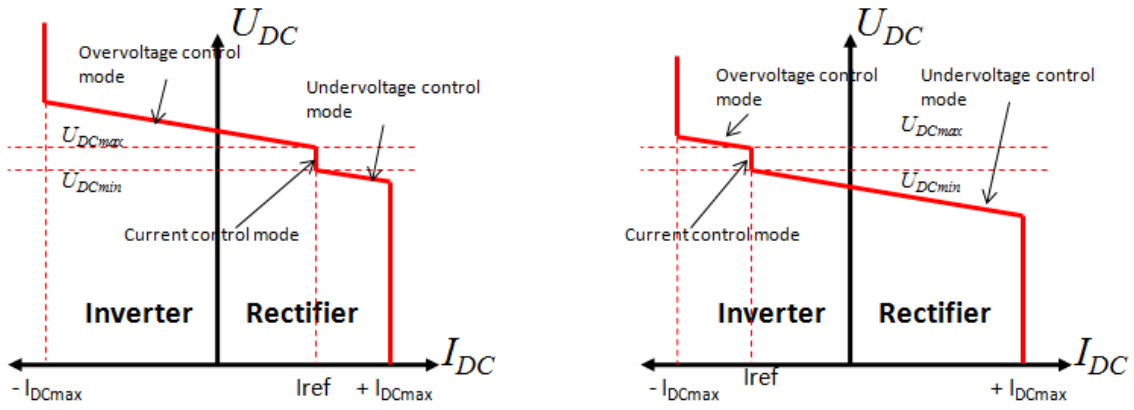

Figure 2-10 Left: Operating characteristic of a current regulated rectifier. Right: Operating characteristic of a current regulated inverter.

2.5.3 Line Current Limiter

This is a task that is out of the scope of this thesis. In AC systems, basically, line overloads are prevented rescheduling the output power of generators. With the help of FACTS devices, line loading in AC grids can be controlled by changing the effective impedance of the line, or which is the same, controlling the voltage across to which the line is exposed.

In DC systems, one way to control current in the DC grid could be to control the voltage across the line. This could be done making a converter to regulate the voltage at one of the line ends so that, the voltage difference across the line results in a current below the current limit. This should be analyzed exhaustively since setting a converter to control DC voltage means that it won't control the power through it, possibly leading to reach the converter current limit, which could lead to further consequences.

Another way to control the line current could be to connect in series DC/DC converter, but this would make the DC grid more expensive and less efficient.

2.5.4 Power - Voltage Operating Curves

It is usual that system operators in charge of DC systems, similar to AC system, have the will of scheduling power rather than current. In this case, the control curve will look as shown in Figure 2-11.

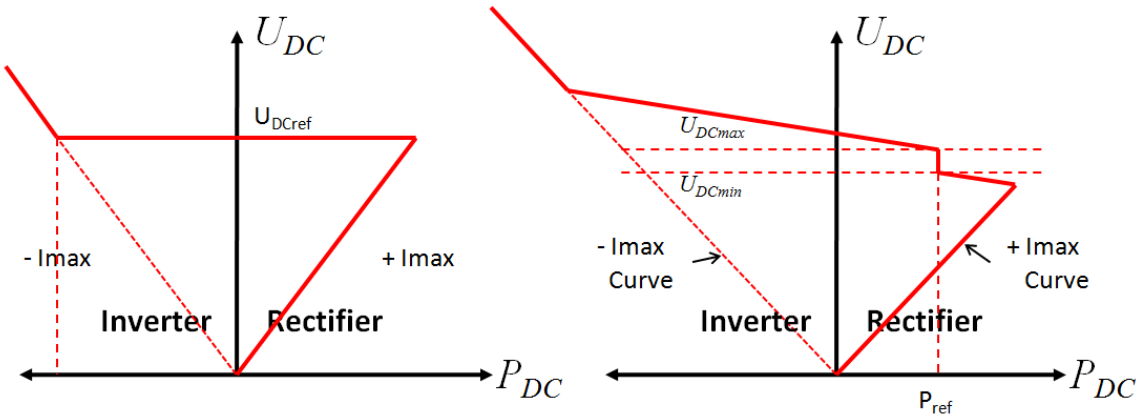

Figure 2-11 Left: Operating characteristic of DC voltage regulating converter. Right: Operating characteristic of a power regulating rectifier.

From these curves, the following equations, that describe the steady stated behavior of the converter, can be found:

Voltage regulating converter

$$U_{DC} = U_{DCref} \tag{2.1}$$

Under voltage control mode

$$P = P_{ref} - \left(U_{DC} - U_{DC\,min}\right)/k \tag{2.2}$$

Over voltage control mode

$$P = P_{ref} - \left(U_{DC} - U_{DC\,max}\right)/k \tag{2.3}$$

Power control mode

$$P = P_{ref} \tag{2.4}$$

Where:

U_{DC} : Measured DC voltage
P : Measured power
P_{ref} : Power reference set-point
U_{DCmax}, U_{DCmin} : Maximum voltage and minimum voltage, respectively, for power control mode.
k : Power - voltage slope

***U_{DCmax}* and *U_{DCmin}*:** Depending on these parameters it can be determined how stiff the input or output power is. If U_{DCmax} is very high and U_{DCmin} is very low, then, the power demanded by the converter will be kept constant. On the other hand, if there is a small margin between U_{DCmax} and U_{DCmin}, then, the converter will be more likely to contribute to the DC voltage control when abnormal voltages occur.

***k*:** This is the slope of the curve in the overvoltage and undervoltage mode. It determines how much the converter is going to contribute to the power balance. If it is big, it means that the converter will contribute very little to the DC voltage regulation. If it is small, the curve will be flatter and then, the contribution to the DC voltage regulation will be higher.

***P_{ref}*:** This parameter defines the power that is going to be put in or out the DC grid under normal conditions. If positive, the converter is operating as rectifier; if negative, it is working as inverter.

It is important to note that the values of U_{DCmin} and U_{DCmax} should ensure that only converters designated to regulate DC voltage comply with the task of controlling voltage. If the selection of U_{DCmin} and U_{DCmax} is very narrow, converters that control power in normal conditions could start controlling voltage in any event, even if voltage regulating converters have still capacity to balance the power in the DC system. From these, typical values could be U_{DCmin} equal to 0.95 p.u, and U_{DCmax} equal to 1.05 p.u.

However, if the DC system has no ability to balance the power (there is no voltage regulating converter) the power controlling converters will start controlling voltage when U_{DCmin} or U_{DCmax} are exceeded. This means that, in absence of DC voltage regulating converters, admissible operating voltage range in the DC system should be allowed to be even wider. In this thesis, a voltage range of 0.9 – 1.1 p.u. will be used as a limitation when there is no voltage regulating converter present in the DC system.

2.6 Operation in Parallel with AC grids

We have seen in previous sections a series of control strategies that help to ensure the secure operation of DC grids. One important thing to consider is that DC grid dynamics, mainly driven by capacitor dynamic, is fast compared to electromechanic AC dynamics. In case of converter outages, the DC system will demand fast changes in power that will affect the performance of AC systems.

In normal conditions, there should be at least one converter that sets the DC voltage in the grid, which can be called the slack bus in the DC system. The impact on the respective AC system is that under contingencies, this converter would be the one in charge of balancing the power in the DC grid. The AC system connected to this converter should have enough reserve available to cover this requirement. Also, since DC dynamics requires fast actions, the respective AC systems should be strong enough, to remain stable after fast changes.

If the DC voltage regulating converter is suddenly disconnected, then the others will have to change their power settings in order to balance the power in the DC grid. Again, it should be analyzed which AC grids are able to collaborate with the stability of the DC grid and to which extent. With this analysis, parameters like U_{DCmax} and U_{DCmin} and the curve slopes can be set properly.

In [9] it is stated that perturbations in one AC system connected to a DC grid shouldn't have a major influence in the other connected AC system. So, if a fault occurs in one AC system, the power transfer should be barely affected. Phenomena like power oscillations in one AC system shouldn't be transmitted to other AC systems, for instance.

Also in [9] it is mentioned the possibility of using the DC grids for issues like frequency regulation and power oscillation damping. Frequency regulation will be discussed further in Chapter 4 and a proposed scheme will be tested in Chapter 5. Power oscillation damping won't be analyzed in this thesis.

In Chapter 5, a set of simulations will be carried out in order to investigate these aspects presented here. Next, in Chapter 3 and 4, control issues will be presented.

Chapter 3

System Element Modeling and Software

The modeling of power system elements for computing purposes depends on the time frame in which the analysis is intended to be done. As an example, electromagnetic transient simulations are aimed to analyze events that last in the range of micro and milliseconds, so models should consider high frequency representation. Transient stability simulations are aimed to analyze events in the range of seconds to tens of seconds, so in this case, fundamental frequency representation is enough for network models. Load flow simulations, on the other hand, are to analyze steady state where every dynamic process has stopped changing in time, so algebraic equations are enough rather than differential equations as the former cases [21].

In this chapter, the modeling of the system elements, i.e. VSC-HVDC terminal model, reactor model, and power system element models, is presented. The software tool used for the modeling task, SIMPOW, also is briefly introduced in this Chapter.

3.1 Model Objectives and Validity

The objective of the modeling task is to develop a simple VSC-HVDC model that helps to analyze, in the AC system, electromechanical dynamics and frequency regulation, and, in the DC system, DC grid dynamics.

In the case of AC systems, since the objective is to analyze the electromechanical behavior, the time frame of the models is in the order of seconds. Due to this, transmission lines, for instance, are modeled as π sections [21], excluding the electromagnetic transients due to oscillations between capacitances and inductances. Transformer, reactors and capacitors in the AC systems are modeled as reactances. As a consequence, grid equations are complex algebraic equations without derivatives.

Moreover, in long-term stability simulations, voltages and currents are modeled as phasors rather than time varying signals. This, certainly, reduces the simulation time when compared with the use of sinusoidal sources since it would allow the simulation program to use adaptive steps for solving the differential equations of the machines. The

use of phasors means that results are relevant only for the fundamental frequency. Positive sequence is used for the modeling task so only balanced events are simulated.

In the DC system, since DC voltage regulation is the aim of the analysis, the model should include dynamic behavior of capacitor and inductances of the DC grid. In this case, then, DC grid equations are composed of differential equations of capacitances and inductances.

This model is valid to analyze electromechanic dynamic behavior in the AC system, and DC grid dynamic behavior following a balanced event. It is not intended for faults since it would imply detailed modeling of, for instance, power electronic devices, filters, smoothing reactors, controller, etc. Control issues are also concerned by the fact of neglecting electromagnetic transients in the AC grid, since things like data processing, PLL, firing circuits, should be designed to be accurate for network transients.

3.2 SIMPOW and DSL Language

SIMPOW is owned and developed by STRI AB. According to the modeling objectives stated above, SIMPOW is suitable for the simulation and modeling tasks demanded by this thesis. One powerful feature of SIMPOW is the availability of an own modeling language (DSL) to create new “processes” according to the user’s needs.

For dynamic simulation, SIMPOW counts on two modules: transient stability module, or TRANSTA, and instantaneous value calculation module, or MASTA. TRANSTA will be used for this thesis since this module uses phasors for AC sytems, considering machine dynamics together with exciters and governors, while in the DC system it takes into account differential equations for capacitor and inductors.

Power flow module in SIMPOW is used to perform steady state simulations and to give initial values to the dynamic simulations.

3.2.1 DSL (Dynamic Simulation Language)

In SIMPOW, the simulation models consist of processes that interact among them [22] exchanging information through connecting variables or by connections with AC or DC nodes [22]. Basically, with DSL, the user can create user-defined processes that will communicate with standard processes in SIMPOW or with other DSL processes. For detailed information about DSL see [22].

Something important is that, in SIMPOW, processes can only inject currents and not set voltage at nodes since SIMPOW solver calculates voltages at all nodes by the condition that the sum of all currents injected to the node must be equal to zero. Therefore, the model “injects” current at the buses where it is connected.

3.3 VSC-HVDC Terminal model

In Figure 3-1 and Figure 3-2, the VSC-HVDC terminal model corresponds to the elements inside the dotted box. All inside the box will be modeled with the help of DSL. Elements outside the box are standard models in SIMPOW.

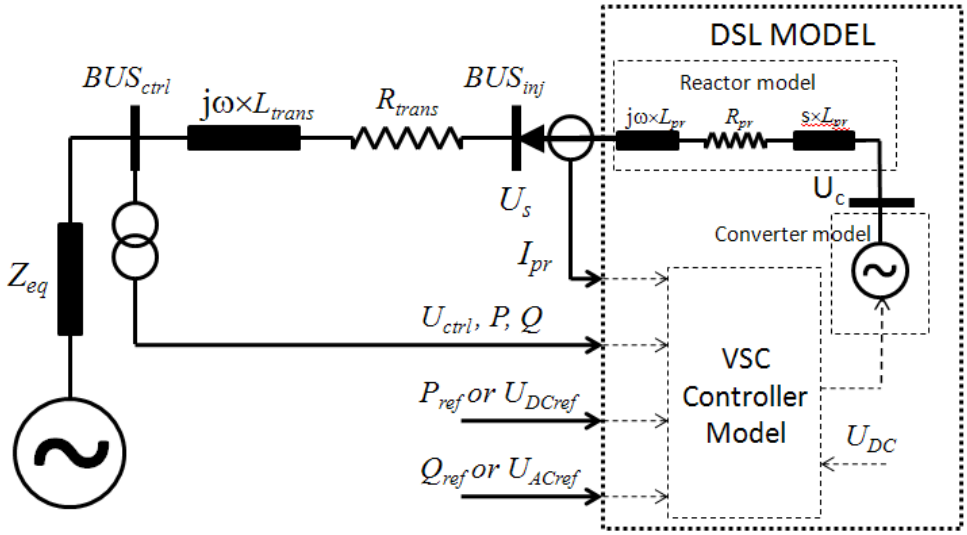

Figure 3-1 AC side of the converter model

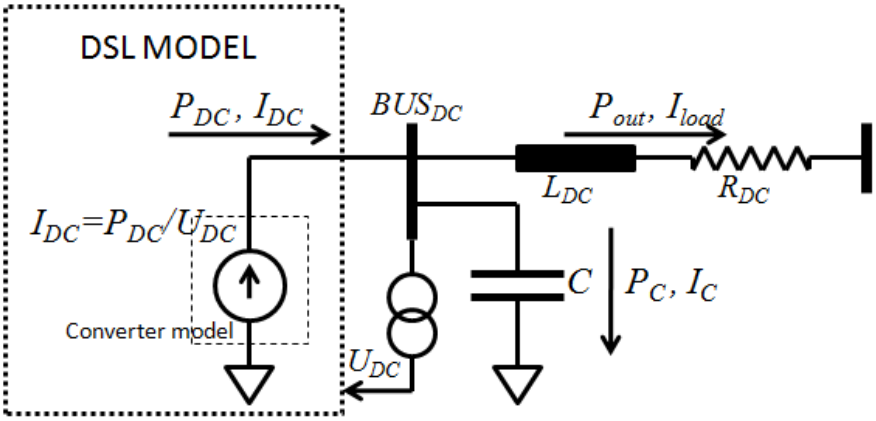

Figure 3-2 DC side of the converter model

Two DSL processes are developed, a VSC-HVDC terminal model for power flow simulations, and another one for dynamic simulations. The former is used to initialize the latter.

All the AC and DC variables used in the model equations are in p.u. Positive sequence variables pre-calculated by SIMPOW are used for AC variables.

Single pole converters will be modeled. The results can be extended to two pole converters.

Inside the VSC-HVDC terminal model three blocks can be identified: the series reactor, the converter, and the controller. In the next Section, converter and reactor models are presented. Controller model is presented in Chapter 4.

3.3.1 Converter model

The converter is modeled, on the AC side, as an ideal positive-sequence voltage source, where the magnitude and the angle is controlled according to the controller output. As mentioned previously, voltages are modeled as phasors so the switching pattern is completely neglected.

In the DC side, the converter is modeled as a current source, whose magnitude is as shown in Figure 3-2. Since switching pattern is neglected, harmonics due to this are not present. In Figure 3-2 it can be seen that at the node BUS_{DC} a capacitor is connected. This capacitor might represent only the capacitor of the DC link, or might include also the capacitance of the cable or overhead line. Capacitor equation is not included in the DSL model. Instead, the standard model from SIMPOW is used.

One important relationship in the converter is energy conservation which means that power in the AC side, should be the same as the DC side. From that, if converter losses are neglected, the expression for the injected DC current is:

$$I_{DC} = -re\left\{\overline{U}_C \times \overline{I}^{*}_{pr}\right\} \Big/ U_{DC} \tag{3.1}$$

Where:

I_{DC} : DC current injected at BUS_{DC} in p.u.
U_{DC} : DC voltage at BUS_{DC} in p.u.
$\overline{U}_C$: Line to line positive sequence voltage at the converter AC side in p.u.
$\overline{I}^{*}_{pr}$: Conjugate of positive sequence reactor current in p.u.

Another important relationship is the one between U_{DC} and U_C (from Figure 3-1 and 3-2). If pulse width modulation technique is used, the relationship between U_{DC} and U_C, for bipolar system, could be as follows:

$$U_C = m_a \sqrt{\frac{3}{2}} \frac{U_{DC}}{2} \times \frac{U_{DC,BASE}}{U_{AC,BASE}} \tag{3.2}$$

Where:

U_C : Line to line voltage (magnitude) at converter AC side in p.u.
m_a : Modulation index, between 0 and 1 in linear range.
$U_{DC,BASE}$: Voltage base of the converter DC side in kV
$U_{AC,BASE}$: Voltage base of the converter AC side in kV

If overmodulation is allowed then m_a will be between 0 and $4/\pi$ [23]. Considering only one pole $U_{DC}/2$ can be replaced by U_{DC}. Then, the followed relationship will be included in the DSL model.

$$0 \le U_C \le \frac{4}{\pi}\sqrt{\frac{3}{2}}U_{DC} \times \frac{U_{DC,BASE}}{U_{AC,BASE}} \tag{3.3}$$

3.3.2 Reactor model

A reactor is included as shown in the Figure 3-1. The Laplace term "s×L_{pr}" is included to use a PI controller and investigate aspects like bandwidth of the inner current controller and outer controller. Equation (3.4) shows the series reactor equation.

$$L_{pr}\frac{d\bar{I}_{pr}}{dt} = \bar{U}_C - \bar{U}_S - j\omega L_{pr}\bar{I}_{pr} - R_{pr}\bar{I}_{pr} \tag{3.4}$$

Where:

$\bar{I}_{pr}$	: Positive sequence reactor current in p.u.
$\bar{U}_S$	: Voltage at the bus BUS_{inj} in p.u.
L_{pr}	: Reactor inductance in p.u.
R_{pr}	: Reactor resistance in p.u.
ω	: Angular speed

As explained in Section 3.2.1, in SIMPOW, it is not possible to set directly voltage values to a node, but only to inject current. The reactor model will be useful in order to get the current I_{pr} as a result the voltage U_C applied to one end of the reactor.

3.4 Modeling of Power System Elements

All the other elements in the AC and DC system are from the standard library of SIMPOW. Following a very brief description of every element used in the simulations is presented.

Transmission Lines

Transmission lines are modeled as π sections, with a resistance in series with a reactance, and a conductance and susceptance in shunt. The same applies for DC lines and DC cables, with the difference that differential equations for capacitances and inductances are considered

Transformers

Transformers are modeled as an ideal transformer in series with a resistance and reactance. Two, three winding transformer models are available. Tap changers are also available in the models.

Loads

Voltage and frequency dependent models are available. The basic equations are as follow:

$$P_{LOAD} = P_0 \times \left(\frac{V}{V_0}\right)^{MP} \left(\frac{f}{f_0}\right)^{NP} \tag{3.5}$$

$$Q_{LOAD} = Q_0 \times \left(\frac{V}{V_0}\right)^{MQ} \left(\frac{f}{f_0}\right)^{NQ} \tag{3.6}$$

Synchronous Machines

Synchronous machines are type 1 in SIMPOW. Detail description of the model can be found in [22]. Exciter and governor models are included.

Capacitor

Capacitor for AC systems is modeled as a capacitive reactance that injects reactive power to the node where it is connected. For DC systems, capacitor considers the following equations:

$$i_C = C\frac{dv_C}{dt} \tag{3.7}$$

Where:

i_C : Current through the capacitor
v_C : Voltage across the capacitor
C : Capacitance

3.5 Load Flow Modeling

A different DSL code for load flow simulations is developed. In this case, SIMPOW adds the algebraic equations from the DSL model to the load flow formulation and solves all the equations together. Equations for the load flow model are in per unit.

In the Figure 3-3, I_{pr} is the positive sequence current at the controlled bus. The voltage U_{ctrl} is the positive sequence voltage at the controlled bus. The impedance between the

buses BUS_{inj} and BUS_{ctrl} may represent, for instance, a transformer. Different from the dynamic model, a reactor model is not included (not needed) for the power flow model.

The load flow model is mainly used to initialize the dynamic simulations. Load flow studies could be done with this model; however, it must be taken into account that current limiters and AC voltage dependence on DC voltage are not modeled.

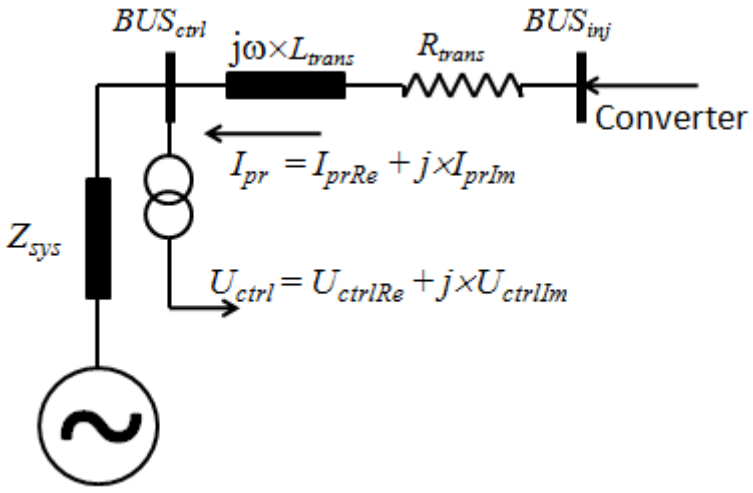

Figure 3-3 AC side of the system for the converter model

3.5.1 Active power control

This corresponds to VSC-HVDC terminals that are set to control power instead of controlling DC voltage. The active power control is defined according to the curves explained in the Section 2.5. So, re-writing the equations we can get the following for the load flow formulation:

For overvoltage control mode ($U_{DC} > U_{DCmax}$):

$$U_{DC} = U_{DC\,max} - k \times \left(re\left\{ \overline{U}_{ctrl} \times \overline{I}_{pr}^{*} \right\} - P_{ref} \right) \tag{3.8}$$

For undervoltage control mode ($U_{DC} < U_{DCmin}$):

$$U_{DC} = U_{DC\,min} - k \times \left(re\left\{ \overline{U}_{ctrl} \times \overline{I}_{pr}^{*} \right\} - P_{ref} \right) \tag{3.9}$$

For power control mode:

$$P_{ref} = re\left\{ \overline{U}_{ctrl} \times \overline{I}_{pr}^{*} \right\} \tag{3.10}$$

Where re{.} stands for the real part of a complex variable.

3.5.2 Reactive power control

This corresponds to VSC-HVDC terminals that control reactive power. The equation to be included in the load flow model is:

$$Q_{ref} = im\left\{\overline{U}_{ctrl} \times \overline{I}^{*}_{pr}\right\} \tag{3.11}$$

Where im{.} stands for the imaginary part of a complex variable.

3.5.3 DC voltage control

This corresponds to VSC-HVDC terminals that are set to regulate DC voltage. According to this, the equation to be included in the load flow model is:

$$U_{DC} = U_{DCref} \tag{3.12}$$

3.5.4 AC voltage control

Instead of controlling the reactive power at the controlled bus, it can be chosen to regulate the AC voltage at the controlled bus. Then, the equation included for the power flow formulation is:

$$\left|\overline{U}_{ctrl}\right| = U_{ACREF} \tag{3.13}$$

3.5.5 Linking DC system with AC system

The link between both systems is the power transformer. The active power from the AC side of the converter must be the same as the power transferred to the DC side. According to this, the equation included in the load flow formulation is:

$$I_{DC} = -re\left\{\overline{U}_{C} \times \overline{I}^{*}_{pr}\right\} \Big/ U_{DC} \tag{3.14}$$

Chapter 4

Control System Modeling

In this chapter control system modeling is presented. The modeling will be based on [15] and [24]. One of the main assumptions stated in the previous chapter is that phasors will be used instead of sinusoidal time varying signals. This assumption allows the use of positive sequence for the controller equations.

This chapter will start with the derivation of the control system, and, at the end, an analysis of the performance of the DC voltage controller will be presented.

4.1 *Dq* Transformation

The *dq* transformation is widely used in control of converters [15], [24], [25]. Some advantages are that this transformation allows analyzing DC quantities, which are simpler rather than AC. Another advantage is that it allows using integrators that reduce to zero the error signal [25].

To arrive to the *dq*-frame, first we have to transform time-varying signals into vectors with the $\alpha\beta$ transformation. According to [26], the formula is:

$$v(t) = v_\alpha + jv_\beta = K\left(v_1(t) + v_2(t)e^{j2\pi/3} + v_3(t)e^{j4\pi/3}\right) \tag{4.1}$$

If balanced three-phase voltages are expressed with the Euler representation for cosines they will be as follow:

$$v_1(t) = V\cos(\omega t - \phi) = V\frac{e^{j(\omega t-\phi)} + e^{-j(\omega t-\phi)}}{2} \tag{4.2}$$

$$v_2(t) = V\cos(\omega t - \phi - 2\pi/3) = V\frac{e^{j(\omega t-\phi-2\pi/3)} + e^{-j(\omega t-\phi-2\pi/3)}}{2} \tag{4.3}$$

$$v_3(t) = V\cos(\omega t - \phi + 2\pi/3) = V\frac{e^{j(\omega t-\phi+2\pi/3)} + e^{-j(\omega t-\phi+2\pi/3)}}{2} \tag{4.4}$$

Then replacing in (5.1)

$$v_\alpha + jv_\beta = K\left(\frac{3Ve^{j(\omega t-\phi)} + Ve^{-j(\omega t-\phi)} + Ve^{-j(\omega t-\phi+2\pi/3)} + Ve^{-j(\omega t-\phi-2\pi/3)}}{2}\right) \tag{4.5}$$

Since the last three terms represent a balanced system, the sum of them will be zero, then:

$$v_\alpha + jv_\beta = K\left(\frac{3}{2}Ve^{j(\omega t-\phi)}\right) \tag{4.6}$$

If *K* equal to 2/3 is selected, corresponding to an amplitude invariant transformation, then:

$$v_\alpha + jv_\beta = Ve^{j(\omega t-\phi)} = V\left(\cos(\omega t-\phi) + j\sin(\omega t-\phi)\right) \tag{4.7}$$

In this equation, the term ωt means that the result in $\alpha\beta$-frame is a vector that is rotating with angular frequency equal to ω.

If the following relationship to change the $\alpha\beta$-frame to the rotating *dq*-frame is finally used:

$$v_{dq} = v_{\alpha\beta}e^{-\omega t} = Ve^{j(\omega t-\phi)}e^{-\omega t} = Ve^{j(-\phi)} \tag{4.8}$$

On the other hand, if we use phasors to represent the sinusoidal voltages (4.2), (4.3), and (4.4) then:

$$\bar{v}_1 = V\angle -\phi \tag{4.9}$$

$$\bar{v}_2 = V\angle -\phi - 2\pi/3 \tag{4.10}$$

$$\bar{v}_3 = V\angle -\phi + 2\pi/3 \tag{4.11}$$

And the positive sequence voltage will be equal to:

$$\bar{v}_p = \frac{1}{3}\left(\bar{v}_1 + a\bar{v}_2 + a^2\bar{v}_3\right) \tag{4.12}$$

With $a = 1\angle 2\pi/3$

Replacing (4.8), (4.9), (4.10) in (4.11):

$$\bar{v}_p = V\angle -\phi = Ve^{j(-\phi)} \tag{4.13}$$

It can be seen that equations (4.8) and (4.13) are the same, under the consideration that phasors are balanced. This means that the use of positive sequence is appropriate.

Similar to [15] and [24] the controller uses *dq*-frame. The voltage reference will be the voltage U_{ctrl} at controlled bus BUS_{ctrl} (see Figure 4-1). In this case, the *dq* coordinate system will be oriented so that the positive sequence voltage phasor U_{ctrl} is aligned to the *q* axis as shown in the Figure 4-1 [24]. The other phasors will use this *dq* coordinate system.

Since phasors are used, a PLL block to determine the rotation angle is not needed, and, instead, the angle from the positive sequence voltage U_{ctrl}, θ_{ctrl} is taken directly. So, every positive sequence phasor used (currents and voltages) is rotated over an angle $\pi/2 - \theta_{ctrl}$ in order to get the voltage phasor U_{ctrl} aligned to the q axis.

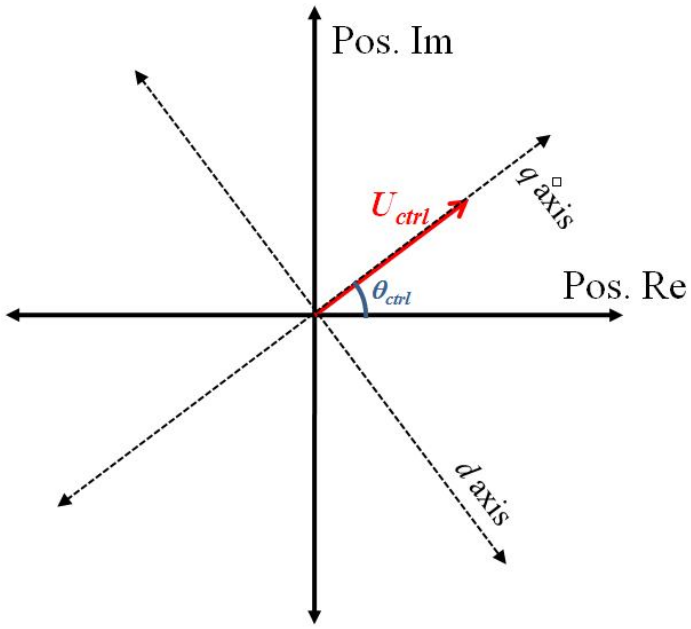

Figure 4-1 Transformation from positive sequence to *dq* coordinate system

The controlled voltage in the *dq*-frame is then:

$$\overline{U}_{ctrl}^{dq} = U_{ctrl}^{d} + jU_{ctrl}^{q} = e^{j(\pi/2-\theta_{ctrl})}\left|\overline{U}_{ctrl}\right|\angle\theta_{ctrl} = j\left|\overline{U}_{ctrl}\right| \tag{4.14}$$

Then:

$$U_{ctrl}^{d} = 0, \text{ and } \quad U_{ctrl}^{q} = \left|\overline{U}_{ctrl}\right| \tag{4.15}$$

The current I_{pr} and voltage U_S used in the controller model are in the *dq*-frame obtained as follow:

$$\overline{I}_{pr}^{dq} = e^{j(\pi/2-\theta_{ctrl})}\overline{I}_{pr} \tag{4.16}$$

$$\overline{U}_{S}^{dq} = e^{j(\pi/2-\theta_{ctrl})}\overline{U}_{S} \tag{4.17}$$

4.2 Inner Current Controller

As was specified in the previous Section, converter controller will use the *dq*-frame. Similar to [15] and [24] a proportional-integral controller is used for the current controller, together with a feed-forward voltage U_{ctrl} , and a cross-coupling compensation block.

According to this, the equations for the current controller in the Laplace domain are [24]:

$$U_C^d = U_{ctrl}^d + \omega L_{pr} I_{pr}^q + \left(k_p + \frac{k_i}{s}\right)\left(I_{prREF}^d - I_{pr}^d\right) \tag{4.18}$$

$$U_C^q = U_{ctrl}^q - \omega L_{pr} I_{pr}^d + \left(k_p + \frac{k_i}{s}\right)\left(I_{prREF}^q - I_{pr}^q\right) \tag{4.19}$$

Usually U_{ctrl} is the same than U_S (see Figure 3-1) since the control is done at the reactor end. If that is assumed, the following block diagram can be derived:

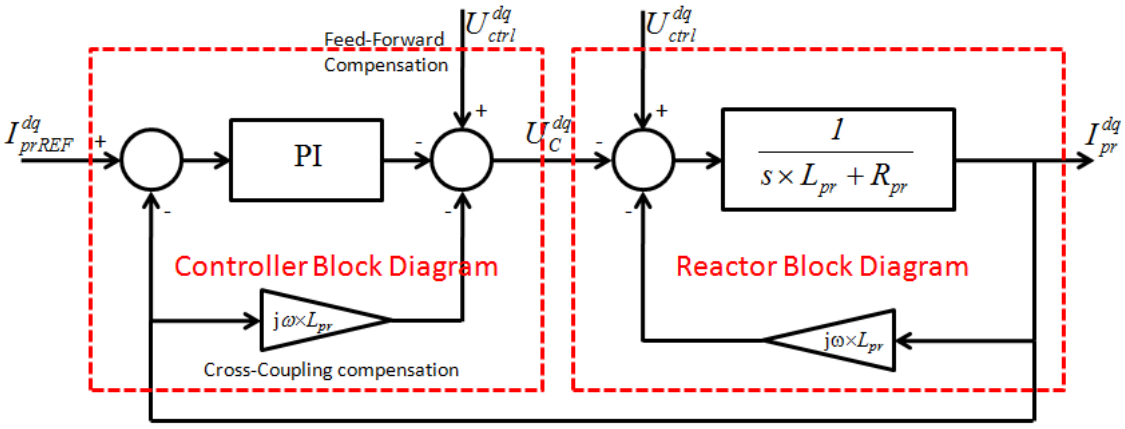

Figure 4-2 Block diagram of the reactor plus controller

In the implemented model, the proportional (k_p) and the integral (k_i) factors could be any value. However, k_p and k_i could be selected in such a way that the equivalent open-loop transfer function is a low pass filter with bandwidth equal to α (see Figure 4-3). In this case, k_p and k_i will get the following values:

$$k_p = \alpha \times L_{pr} \tag{4.20}$$

$$k_i = \alpha \times R_{pr} \tag{4.21}$$

In this model, the output voltage of the converter, U_C, is directly applied to the reactor terminal, after being rotated back over an angle $\pi/2 - \theta_{ctrl}$ to get the positive sequence value. So, there is no time delay from the controller output to the reactor terminal.

If parameters are perfectly matched then the block diagram would be:

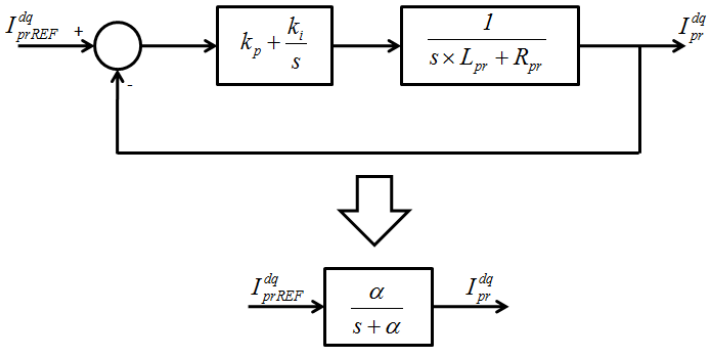

Figure 4-3 System simplified if perfectly matched parameters

A current limiter should be implemented before the reference current goes to the controller in order to avoid dangerous values. The current limiter can act in different ways [27], for example keeping active or reactive power constant. As there is very limited energy storage available in an HVDC link, the common approach is to prioritize the transfer of active power. As will be seen later, I^q_{pr} controls the active power and I^d_{pr} controls the reactive power. If I_{rated} is the current limit, then, the limiter could be as follow:

If I^q_{prREF} is greater than I_{rated} then:

$$I^q_{prREF} = I_{rated} \quad and \quad I^d_{prREF} = 0 \tag{4.22}$$

If I^q_{prREF} is lower than I_{rated} but if I^{dq}_{prREF} is greater than I_{rated} then, I^q_{prREF} remains the same and I^d_{prREF} is:

$$I^d_{prREF} = \sqrt{\left(I_{rated}\right)^2 - \left(I^q_{prREF}\right)^2} \tag{4.23}$$

4.3 Outer Controllers

In this Section, the outer controllers, that will control the active power or DC voltage, and, reactive power or AC voltage will be presented. The outputs of the outer controllers are current references that are input for the current controller as will be shown in this Section.

4.3.1 Active power and DC voltage control

Active power control and DC voltage is related to the current I_{pr}^{q}, so this outer controller will determine the current reference in the *q* axis, I_{prREF}^{q}, *as* will be shown. Only one mode can be selected at a time, either active power or DC voltage control. The derivation of the active power and DC voltage controllers are presented next.

If per unit values are used, then complex power at the controlled bus is:

$$S = U_{ctrl}^{dq} \times \left(I_{pr}^{dq} \right)^{*} \tag{4.24}$$

If the controlled voltage is oriented to the q axis, then:

$$U_{ctrl}^{dq} = jU_{ctrl}^{q} \tag{4.25}$$

$$\left(I_{pr}^{dq} \right)^{*} = I_{pr}^{d} - jI_{pr}^{q} \tag{4.26}$$

The active power can be calculated, then, with the following equation:

$$P = U_{ctrl}^{q} \times I_{pr}^{q} \tag{4.27}$$

Making *P* equal to P_{ref} and $I_{pr}^{q} = I_{prREF}^{q}$, then active power controller can be implemented as follows:

$$I_{prREF}^{q} = P_{ref} / U_{ctrl}^{q} \tag{4.28}$$

According to [15] a PI block can be added to the active power controller, so the equation of the active power controller in the Laplace domain is:

$$I_{prREF}^{q} = \frac{P_{ref}}{U_{ctrl}^{q}} + k_{p,P}\left(P_{ref} - P \right) + \frac{k_{i,P}}{s}\left(P_{ref} - P \right) \tag{4.29}$$

Now, for the DC voltage control, let's consider the dynamic of the capacitor:

$$\frac{dU_{DC}}{dt} = \frac{I_C}{C} \tag{4.30}$$

Where (from Figure 3-2):

$$I_C = I_{DC} - I_{load} \tag{4.31}$$

Considering:

$$I_{DC} = I_{pr}^{q} U_{ctrl}^{q} / Udc \tag{4.32}$$

Then re-arranging the expressions (4.30), (4.31) and (4.32) we get:

$$C\frac{U_{DC}}{U_{ctrl}^{q}}\frac{dU_{DC}}{dt} + \frac{U_{DC}}{U_{ctrl}^{q}} I_{load} = I_{pr}^{q} \tag{4.33}$$

So, as can be seen, the DC voltage is dependent on the current I_{pr}^{q}. According to [15], a PI controller can be used to control de DC voltage so the equation in the Laplace domain is:

$$I_{prREF}^{q} = \frac{U_{DC}}{U_{ctrl}^{q}} I_{load} + k_{p,U_{DC}} \left(U_{DCREF} - U_{DC}\right) + \frac{k_{i,U_{DC}}}{s}\left(U_{DCREF} - U_{DC}\right) \tag{4.34}$$

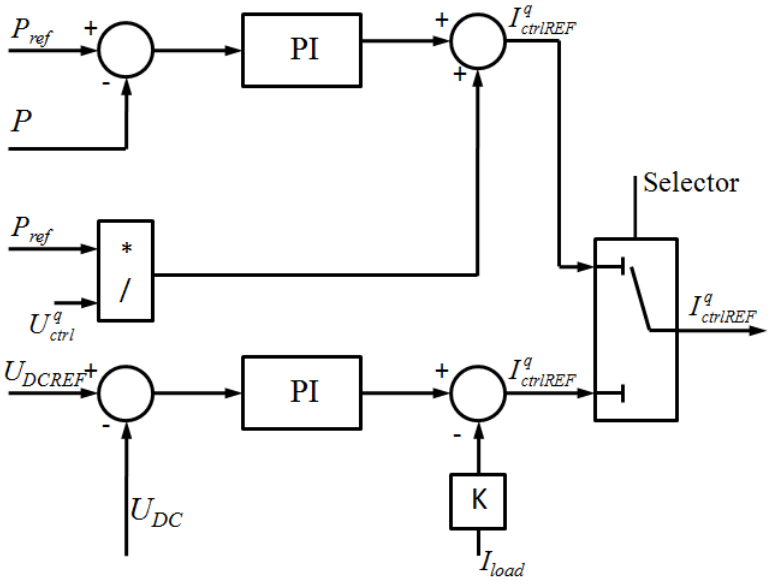

Figure 4-4 Block diagram of the active power and DC voltage controller

4.3.2 Reactive power and AC voltage regulation

The current reference I^d_{prREF} can be obtained from the equation (4.24), (4.25) and (4.26):

$$I^d_{prREF} = Q_{REF} / U^q_{ctrl} \tag{4.35}$$

According to [15] a PI block can be added to the reactive power controller, so the equation of the reactive power controller in the Laplace domain is as follow:

$$I^d_{prREF} = \frac{Q_{REF}}{U^q_{ctrl}} + k_{p,Q}\left(Q_{REF} - Q\right) + \frac{k_{i,Q}}{s}\left(Q_{REF} - Q\right) \tag{4.36}$$

In [15] it is demonstrated that AC voltage is mainly dependent on Q, which as shown in the equation (4.35), is proportional to I^d_{pr}, and then, a PI block is used. The equation of the AC voltage controller in the Laplace domain is as follow:

$$I^d_{prREF} = k_{p,U_{AC}}\left(U^q_{ctrlREF} - U^q_{ctrl}\right) + \frac{k_{i,U_{AC}}}{s}\left(U^q_{ctrlREF} - U^q_{ctrl}\right) \tag{4.37}$$

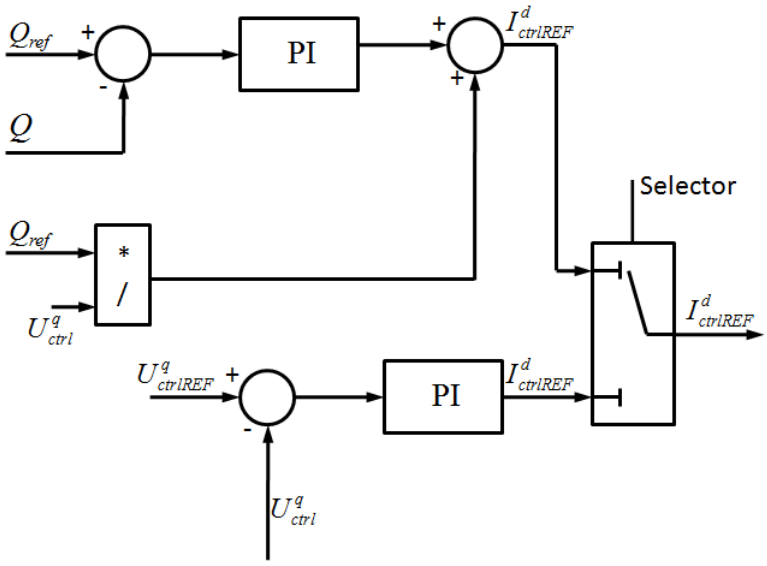

Figure 4-5 Block diagram of the reactive power and AC voltage controller

4.3.3 Proposed control for multi-terminal operation

In Section 2.5, the implementation of active power – voltage curves to control power transmission in a multi-terminal DC grid was presented. In normal operation, one of the converters sets the DC voltage in the DC grid and the rest of the converters will operate at fixed active input or output power. However, under contingencies, the DC voltage at the

DC grid may either decrease or increase; if the power in the DC grid is not balanced the converters will adjust their input or output power to balance the power in the system.

Figure 2-11 shows the proposed control curve where four operating modes are identified. Using the equations (2.2), (2.3) together with the equation (4.29) then, the equations in the Laplace domain are:

Undervoltage control mode:

$$I_{prREF}^{q} = \frac{1}{U_{ctrl}^{q}}\left(\frac{U_{DC\,min} - U_{DC}}{k} + P_{REF}\right) + k_{p,P}\left(\frac{U_{DC\,min} - U_{DC}}{k} + P_{REF} - P\right) + \frac{k_{i,P}}{s}\left(\frac{U_{DC\,min} - U_{DC}}{k} + P_{REF} - P\right) \tag{4.38}$$

Overvoltage control mode:

$$I_{prREF}^{q} = \frac{1}{U_{ctrl}^{q}}\left(\frac{U_{DC\,max} - U_{DC}}{k} + P_{REF}\right) + k_{p,P}\left(\frac{U_{DC\,max} - U_{DC}}{k} + P_{REF} - P\right) + \frac{k_{i,P}}{s}\left(\frac{U_{DC\,max} - U_{DC}}{k} + P_{REF} - P\right) \tag{4.39}$$

Power control mode:

Equation (4.29)

Current limiting mode:

Equation (4.22) or (4.23)

4.4 Analysis of the DC System Dynamic

Typically, the DC capacitor is chosen so that the time constant is 2 ms [28] or 5 – 10 ms according to [22]. The time constant is defined as follow:

$$\tau = \frac{1}{2}\frac{C \times U^{2}}{P_{NOM}} \tag{4.40}$$

Where:

U : Nominal Voltage on the DC side (kV)
P_{NOM} : Nominal Power (MW)
C : Capacitance (μF)

For instance, in [15], a capacitor equal to 75.2 μF per terminal, with a nominal voltage of 160 kV and nominal power of 60 MW, will have a time constant τ equal to 16 ms. It means that, the energy stored in the capacitor will be totally discharged in 16 ms if nominal power is drawn from the capacitor all the time.

In the system shown in Figure 4-6 there are two converters, A and B, where A is controlling the power transfer while B is controlling the DC voltage. Converter A is putting power into the DC grid equal to zero at t = 0. At t = 0.02, the power reference is increased from 0 to 0.5 p.u in the converter A. The output, I^q_{prREF}, of the active power outer controller is determined by equation (4.29)

So, the term $I^q_{prREF} = P_{ref} / U^q_{ctrl}$ indicates that I^q_{prREF} will be immediately changed. This means that, at terminal A, the power will change to the new power reference at the speed of the current controller, which has a bandwidth equal to α.

Let's assume that the speed of the current controller of terminal A is much faster than the speed of the DC voltage controller of terminal B. Since DC voltage is controlled with I^q_{prREF}, it means that, at terminal B, the current I^q_{pr} will take time to change from the original value to the one required to have the DC voltage equal to the reference. So, during the time that DC voltage controller takes to respond to the active power change in terminal A, the capacitor at terminal B will be charged with a power equal to the difference $P_A - P_B$ (From Figure 4-6) until the DC voltage controller starts to respond.

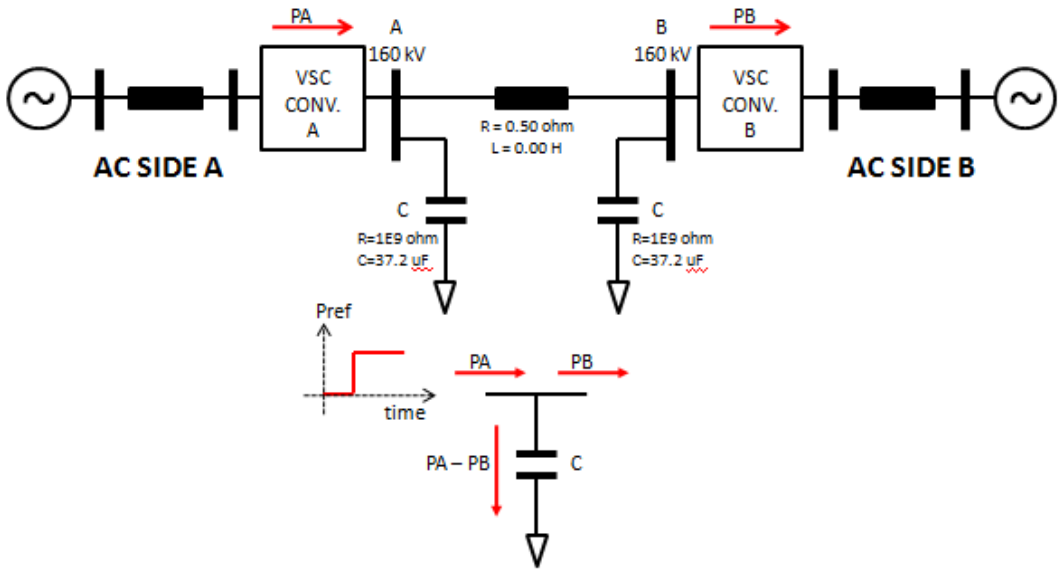

Figure 4-6 Two terminal system.

The change in voltage during the "non-operation" of DC voltage controller will depend on the capacitance. This is, the lower the capacitance (i.e. the smaller the time constant τ), the higher the voltage variation.

It can be seen, then, that there is a relationship between the bandwidth of the DC voltage controller and the time constant of the capacitor. So, if, a sudden change of power occurs, in order not to have large DC voltage variations, the response of the DC voltage controller should be faster than the time constant τ. It means that a higher bandwidth of the DC voltage controller, or a higher capacitance, would improve the dynamic response of the DC link.

4.4.1 Design of the DC voltage controller

In Section 4.3 it was said that a PI controller would be used for the voltage controller. So, the design of the controller, basically, consists of determining the controller parameters, in this case $k_{p,U_{DC}}$ and $k_{i,U_{DC}}$. Since the process is simple (capacitor dynamic), it is possible to carry out an analytical approach to find the parameters.

In [29] and [30] an analysis is made of a DC voltage controller considering a droop control rather than a PI controller for the voltage. The control system analyzed in those studies is as shown in Figure 4-7.

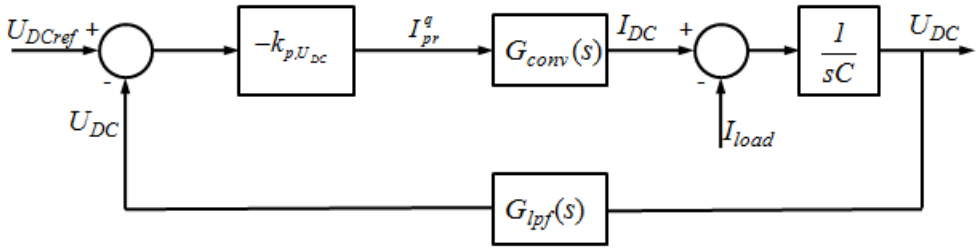

Figure 4-7 Closed-loop control system for control of the DC link voltage [29].

In this thesis, the controller model is simplified, where the switching pattern and the delaying effect of a low pass filter are neglected. However, the delaying effect of the low pass filter is still there and it would, definitively, affect the DC voltage controller performance, so in a more detailed model it must be taken into account. Another difference is that, in this thesis, a proportional-integral control is used instead of only proportional (droop control).

The system used in this thesis is shown in Figure 4-8. There is no low-pass filter for the measured U_{DC} feedback and, integral part is included in the DC voltage controller. The integral part ensures that the voltage will be set equal to the U_{DCref}. One assumption that simplifies the analysis is to consider the speed of the inner current controller very fast compared to the outer controller's bandwidth. If so then:

$$G_{conv}(s) = \frac{U_{ctrl}^{q}(s)}{U_{DC}(s)} \tag{4.41}$$

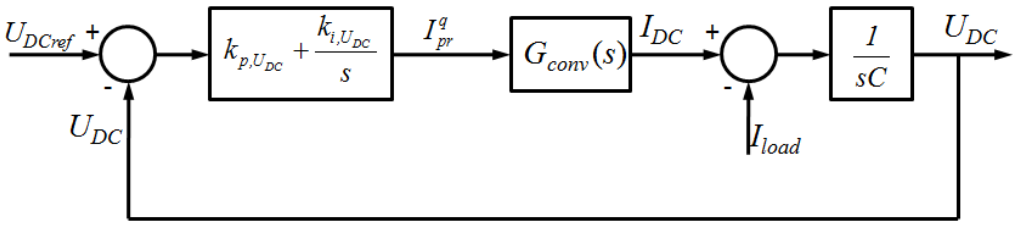

Figure 4-8 Closed-loop control system for control of the DC link voltage used in this thesis

If per unit values are used and assuming that $U_{ctrl}^{q}(t) \approx 1$ p.u. and $U_{DC}(t) \approx 1$ p.u. (i.e. variations of voltages are small) in the time domain, then in the Laplace domain $G_{conv}(s) \approx 1$. With this assumption it can be found that the open loop transfer function is:

$$U_{dc} = \left(\frac{\frac{kp_{udc}}{C} s + \frac{ki_{udc}}{C}}{s^2 + \frac{kp_{udc}}{C} s + \frac{ki}{C}} \right) \times U_{DCref} - \left(\frac{\frac{s}{C}}{s^2 + \frac{kp_{udc}}{C} s + \frac{ki}{C}} \right) \times I_{load} \tag{4.42}$$

Using the final value theorem for Laplace functions, for a step-like change of either I_{load} or U_{DCref}, it can be shown that in steady state $U_{DC} = U_{DCref}$.

Looking at the transfer function we can see that the characteristic polynomial is:

$$p(s) = s^2 + \frac{k_{p,U_{DC}}}{C} s + \frac{k_{i,U_{DC}}}{C} \tag{4.43}$$

This corresponds to the following second order equation:

$$p(s) = s^2 + 2\varsigma\omega_{U_{DC}} s + \omega_{U_{DC}}^2 \tag{4.44}$$

Where:

$\omega_{U_{DC}}$: DC voltage controller's bandwidth

ζ : Damping factor

From those equations we can get $k_{p,U_{DC}}$ and $k_{i,U_{DC}}$ as:

$$k_{p,U_{DC}} = 2C\varsigma\omega_{U_{DC}} \tag{4.45}$$

$$k_{i,U_{DC}} = C\omega_{U_{DC}}^2 \tag{4.46}$$

It was assumed that the outer controller speed is slower than inner current controller, so, the bandwidth, $\omega_{U_{DC}}$, of the DC voltage controller should be smaller than the bandwidth of inner current controller α.

4.4.2 Damping factor effect

In [15] there is a two-terminal example, whose main data are shown in Figure 4-9. In this example, the switching frequency is 2000 Hz, so the inner current controller should be slower. Let's assume a factor 10. That is: $\alpha = 2\pi \times 2000/10 \approx 1250$ rad/s.

The bandwidth of the DC outer controller should be smaller than this, so let's again assume a factor 10: $\omega_{U_{DC}} = \alpha/10 = 125$ rad/s. The damping factor ζ will be varied from 0.5 to 3, in order to see the effects of it.

The following events are simulated:

t = 0 : Simulation starts, converter 1 regulating power equal to zero and converter 2 regulating DC voltage.
t = 0.02 : Converter 1 changes its setpoint to -0.5 p.u (Power from AC to DC side).
t = 0.12 : Converter 1 changes its setpoint to +0.5 p.u (Power from DC to AC side).
t = 0.16 : Simulation stops.

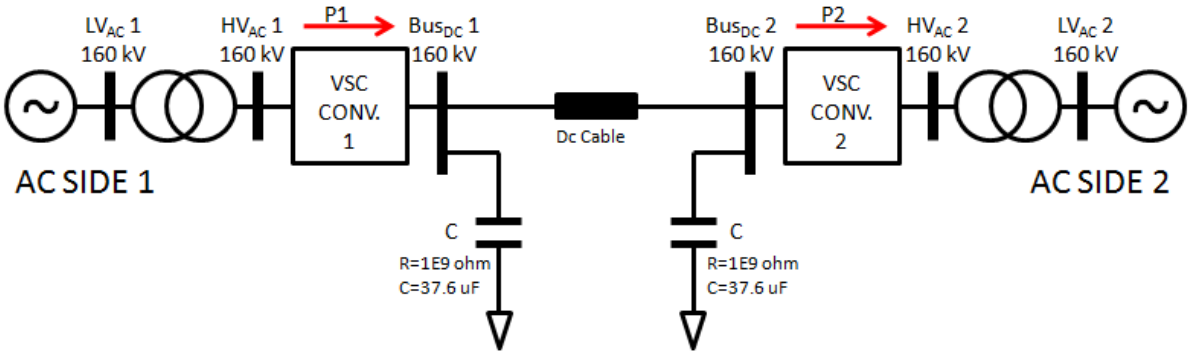

Figure 4-9 Test system used in [15]

Table 4-1 Electrical parameters

Electrical Parameter	Symbol	Physical value
Rated voltage	HV_{AC} 1	150 kV
Rated voltage	HV_{AC} 2	150 kV
DC voltage	Bus_{DC} 1	160 kV
DC voltage	Bus_{DC} 2	160 kV
Rated power	P	60 MW
Reactor inductante	L_{pr}	0.049 H

Reactor resistance	R_{pr}	0.5133 Ω
DC capacitor	C	37.6 μC
System Freq	f	50 Hz
Switching Freq	f_{sw}	2000 Hz

From Figure 4-10 we can see that as long as the damping factor increases, DC voltage oscillations decreases and “peak” voltages also decreases.

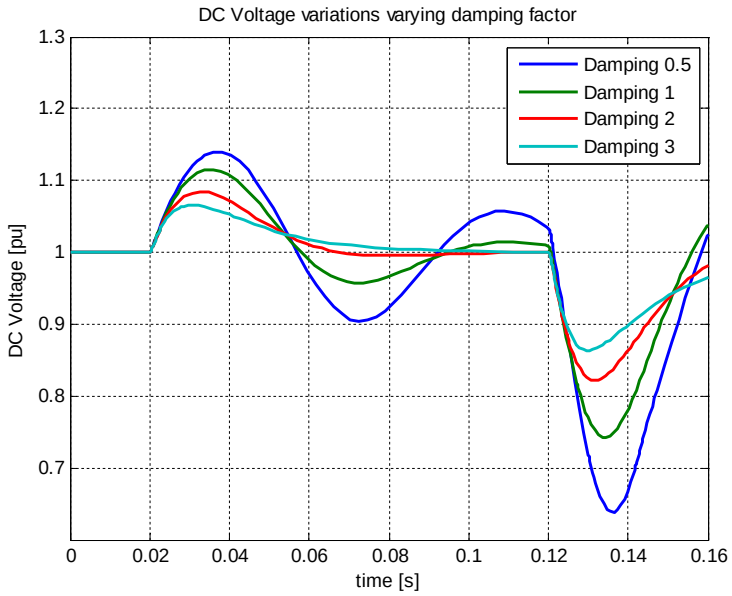

Figure 4-10 DC Voltage with different DC voltage controller damping factor at converter 2

4.4.3 Speed of the DC voltage controller effects

Now, the case when changing the bandwidth of the DC voltage controller will be examined. The bandwidth of the inner current controller is kept the same as specified (1250 rad/s), and the damping factor is set to 3. The bandwidth of the DC voltage controller will be varied from 1/10, 1/5, 1/3, 1/2 and 1 times the bandwidth of the inner current controller.

As can be seen in Figure 4-11, the voltage peaks decrease more effectively and the voltage settles down faster to the steady state. However, it must be noticed that when the DC voltage controller bandwidth is increased, oscillations appear. If the DC voltage controller bandwidth is further increased, the controller will become unstable.

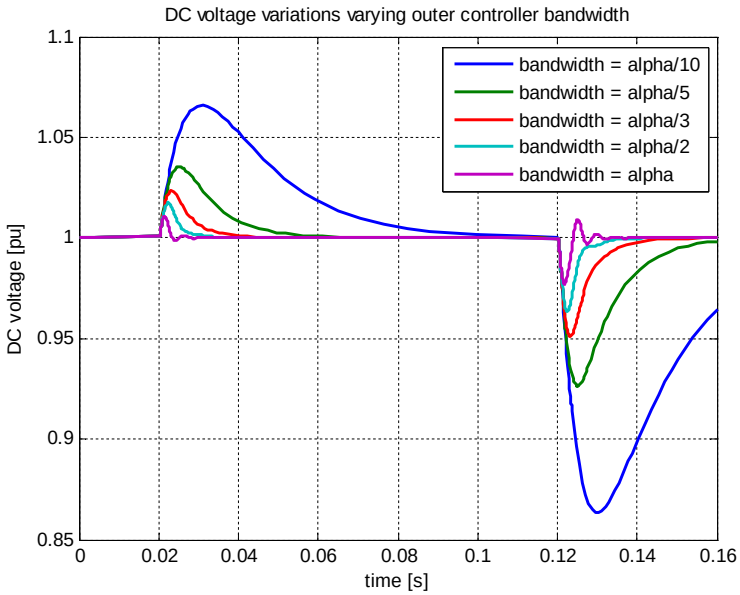

Figure 4-11 DC Voltage with different DC voltage controller bandwidth at converter 2

4.5 Dynamic Analysis of the Proposed Control Strategy

The proposed control method to deal with power unbalances can be analyzed using equations (3.4), (4.19), (4.39), and. One additional equation to be considered is:

$$sCU_{DC} - CU_{DC\,min} = I_{DC} - I_{load} \tag{4.47}$$

From those equations it can be shown that the block diagram is:

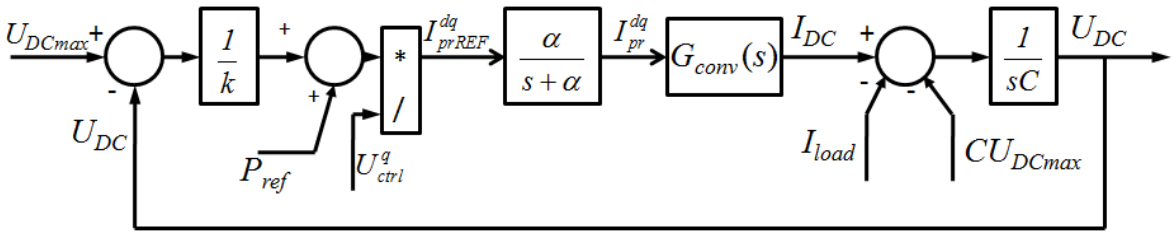

Figure 4-12 Closed-loop control system for overvoltage operating mode

Considering I_{load} = 0, from Figure 4-12 the following expression can be derived:

$$U_{DC} = \frac{\left(1 + \frac{CkU^{q}_{ctrl}}{\alpha}s + CkU^{q}_{ctrl}\right)U_{DC\,max} + kP_{ref}}{\left(\frac{CkU^{q}_{ctrl}}{\alpha}s^{2} + CkU^{q}_{ctrl}s + 1\right)} \tag{4.48}$$

If the speed of the current controller is higher than the capacitor dynamic, the expression (4.48) can be reduced to:

$$U_{DC} = \frac{U_{DC\,max} + kP_{ref}}{CkU_{ctrl}^{q}s + 1} \tag{4.49}$$

So, as long as the speed of the current controller is faster than the capacitor dynamics, the dynamic of the overvoltage control mode (or undervoltage control mode) will be determined by the capacitance *C* and the factor *k*. In Figure 4-13 it can be seen the DC voltage for a simulation which consists of the following events:

t = 0 : Simulation starts, converter 1 regulating power equal to zero and converter 2 regulating DC voltage.
t = 0.02 : Converter 1 changes its setpoint to -0.5 p.u (Power from AC to DC side).
t = 0.12 : Converter 2 is out of service.
t = 0.16 : Simulation stops

In this case, the following parameters were used:

U_{DCmax} = 1.05 p.u
U_{DCmin} = 0.95 p.u
k = 0.05 p.u.

With k in physical values:

k = 0.05×160/100 [kV/MW]

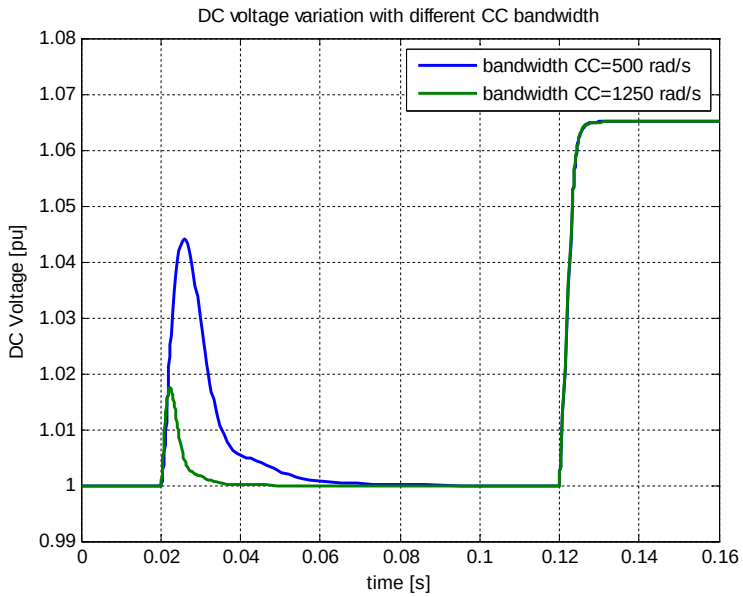

Figure 4-13 DC voltage with different current controller bandwidth at both converters

Two simulations were run for two different current controller bandwidths. The first important conclusion that can be seen is that, although DC voltage regulating converter is put out of service, the DC system remains stable so the proposed controller effectively works in this system.

Secondly, it can be verified that, even though the bandwidth of the current controller has been reduced to less than half the initial bandwidth (1250 rad/s), there is no effect on the behavior of the controller when it goes to overvoltage operation mode. From equation (5.49) the bandwidth of the controller in overvoltage operation mode is:

$$\left(CkU_{ctrl}^{q}\right)^{-1} = \left(2\times 37.6\times 10^{-6}\times 0.05\times \frac{160}{100}\times 150\right)^{-1} = 1108 \text{ rad/s} \qquad (4.50)$$

In this case, two capacitors, from both ends, are considered since in the simulation only the converter 2 is disconnected. In Figure 4-13, a detailed sight of the curves is shown and from that, the rise time can be calculated.

Rise time = 0.1255 – 0.1234 = 0.0021

From the curve, the bandwidth can be calculated as:

Bandwidth = 2.2/0.0021 = 1046 rad/s

Which is a value very close to the theoretical one obtained in equation (4.50)

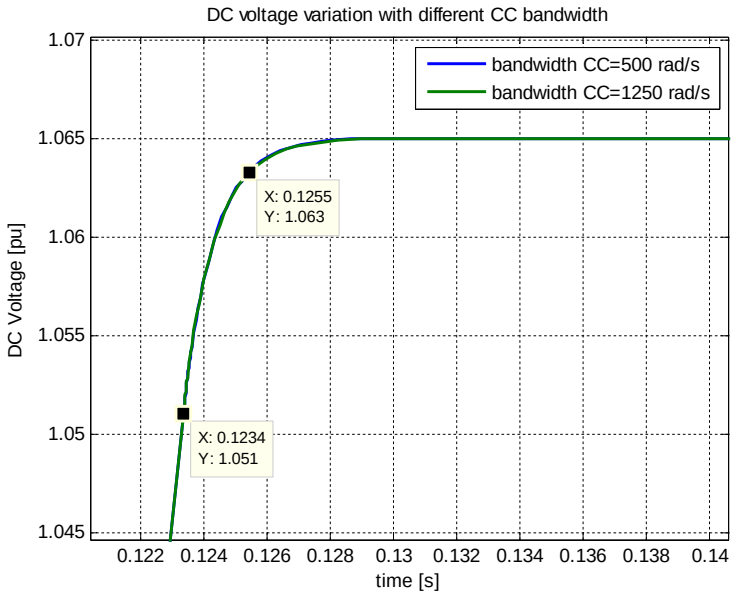

Figure 4-14 Detailed view of Figure 4-13

4.6 Frequency regulation in AC systems connected through a DC grid.

As has been mention in Section 2.3, the operation of an AC system, basically, aims to balance the power flow in the AC system. When an event that implies power unbalance occurs abruptly, frequency will increase or decrease; depending if there is excess or deficit of generation, respectively. When there is a change in frequency, governor actions take places aiming to balance the power in the AC grid. This is called, primary control [16].

In [9] it is said that AC perturbations shouldn't affect the performance of the DC grid, and shouldn't spread their harmful effects to other AC systems. However, the interconnection of AC systems through a DC grid can allow sharing the responsibility of regulating frequency between non-synchronous connected AC systems, spreading the perturbation over more than one system, but mitigating the undesired effects of solving the unbalance locally. The principle used in frequency-droop characteristic [31] can be used to change the power setpoints of converter, as will be shown next.

4.6.1 Frequency regulation scheme

In Figure 4-15 it is shown a scheme of frequency regulation between DC-connected AC systems. In this Figure, converter *A* connects an AC system "*A*" to the DC grid, and converter *B* connects an AC system "*B*" to the same DC grid.

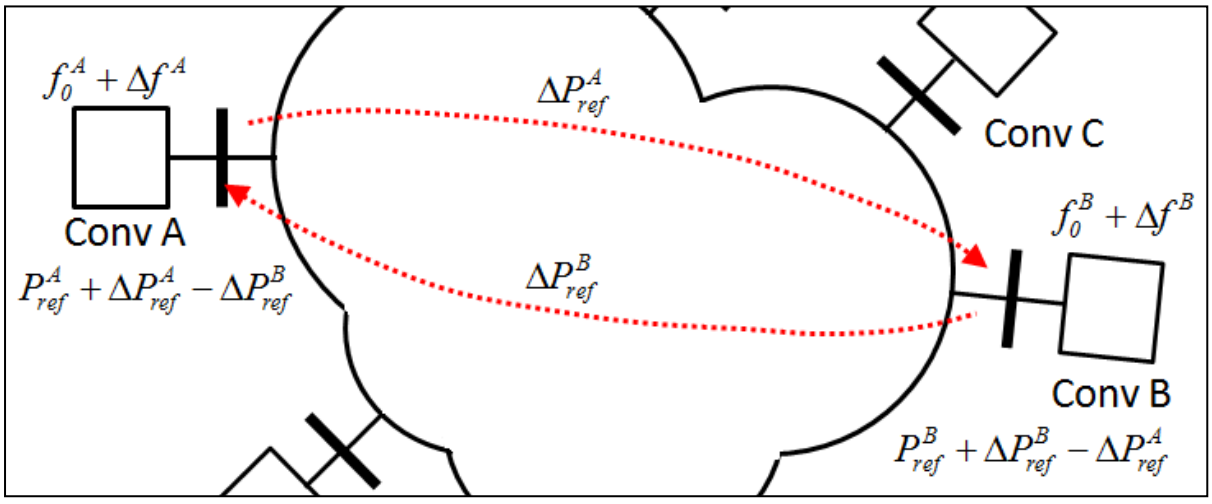

Figure 4-15 Frequency regulation between DC-connected AC systems

f_0^A : Nominal frequency for AC system *A* connected to converter *A*.

Δf^A : Variation in frequency for AC system *A* connected to converter *A* due to a perturbation.

f_0^B : Nominal frequency for AC system *B* connected to converter *B*.

Δf^B : Variation in frequency for AC system *B* connected to converter B due to a perturbation.

P_{ref}^A : Power setpoint at converter *A*.

ΔP_{ref}^A : Change of power setpoint at converter *A* due to a change of frequency in AC system *A*.

P_{ref}^B : Power setpoint at converter *B*.

ΔP_{ref}^B : Change of power setpoint at converter *B* due to a change of frequency in AC system *B*.

In this scheme, a change of the converter's power setpoint as a function of the change in frequency is proposed in a similar way as frequency-droop characteristic of governors. Neglecting losses, in normal conditions, power balance can be expressed with the following equation:

In the AC system *A*

$$P_{Load}^A = P_{Gen}^A + P_{ref}^A \tag{4.51}$$

Where $P_{gen}{}^A$ is the production by all generation in AC network A.

In the AC system *B*

$$P_{Load}^B = P_{Gen}^B + P_{ref}^B \tag{4.52}$$

Where $P_{gen}{}^B$ is the production by all generation in AC network B.

Let's assume a change of load ΔP_{Load}^A in the AC system *A*. This will cause a change of frequency Δf^A, and, as a consequence, will make the output power of generators to change according to the speed-droop characteristic of governors [31]. According to the proposed scheme, the converter will also change its power setpoint by ΔP_{ref}^A due to the variation of frequency. This variation on power setpoint in converter *A* will be transmitted to converter *B*, so that power balance in the DC grid will remain almost unchanged, i.e. the input/output power of the DC voltage regulating converters will remain almost unaffected, except by the change of power losses. If this change of power setpoint is not sent out to any other desired converter, the DC voltage regulating will have to compensate the change of input/output power in the DC grid.

The change of power setpoint in converter *B* will also affect the frequency in the AC system *B*; therefore, if a frequency regulation controller is implemented in converter *B*, it will ask system *A* for a change of power setpoint as well.

Since information has to be exchanged, a communication channel must be established between the selected converters that will cooperate to regulate the frequency.

With these considerations, the power balance equations after a change of load in system *A* are:

$$P_{Load}^{A} + \Delta P_{Load}^{A} = P_{Gen}^{A} + \Delta P_{Gen}^{A} + P_{ref}^{A} + \Delta P_{ref}^{A} - \Delta P_{ref}^{B} \tag{4.53}$$

$$P_{Load}^{B} = P_{Gen}^{B} + \Delta P_{Gen}^{B} + P_{ref}^{B} + \Delta P_{ref}^{B} - \Delta P_{ref}^{A} \tag{4.54}$$

From those equations, we can get the variation of power in system *A* and *B* as:

$$\Delta P_{Load}^{A} = \Delta P_{Gen}^{A} + \Delta P_{ref}^{A} - \Delta P_{ref}^{B} \tag{4.55}$$

$$0 = \Delta P_{Gen}^{B} + \Delta P_{ref}^{B} - \Delta P_{ref}^{A} \tag{4.56}$$

Combining equations (4.55) and (4.56) we can get the following expression:

$$\Delta P_{Load}^{A} = \Delta P_{Gen}^{A} + \Delta P_{Gen}^{B} \tag{4.57}$$

Equation (4.57) means that the variation of load ΔP_{Load}^{A} will not only be compensated by the system *A*'s contribution itself but also with the system *B*'s contribution, at expenses of introducing a perturbation in system *B*.

Equations (4.55), (4.56) and (4.57) can be expressed as a function of frequency variation as follow:

$$\Delta P_{Load}^{A} = \frac{\Delta f^{A}}{R_{Gen}^{A}} + \frac{\Delta f^{A}}{R_{Conv}^{A}} - \frac{\Delta f^{B}}{R_{Conv}^{B}} \tag{4.58}$$

$$0 = \frac{\Delta f^{B}}{R_{Gen}^{B}} + \frac{\Delta f^{B}}{R_{Conv}^{B}} - \frac{\Delta f^{A}}{R_{Conv}^{A}} \tag{4.59}$$

$$\Delta P_{Load}^{A} = \frac{\Delta f^{A}}{R_{Gen}^{A}} + \frac{\Delta f^{B}}{R_{Gen}^{A}} \tag{4.60}$$

By solving equations (4.58) and (4.59) the change of frequency at system *A* and *B* can be determined.

4.6.2 Implementation of the frequency regulation in the VSC controller

The proportional controller of a governor can be used to control the change of power setpoint of the converter. The transfer function is shown in Figure 4-16.

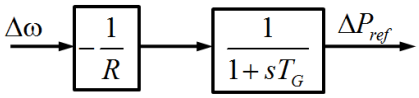

Figure 4-16 Block diagram of the frequency regulation control

Equations for the frequency regulation block are as follow:

$$sT_G \times \Delta P_{ref} = \frac{1}{R}\Delta\omega - \Delta P_{ref} \tag{4.61}$$

Where:

T_G : Time constant of the controller
R : Percent of frequency regulation or droop [31]

The output of this controller ΔP_{ref} is sent to the local power controller and to the power controller of the remote converter selected to contribute with frequency regulation.

The block diagram of the outer power controller (Figure 4-4) can be re-drawn as shown in Figure 4-17.

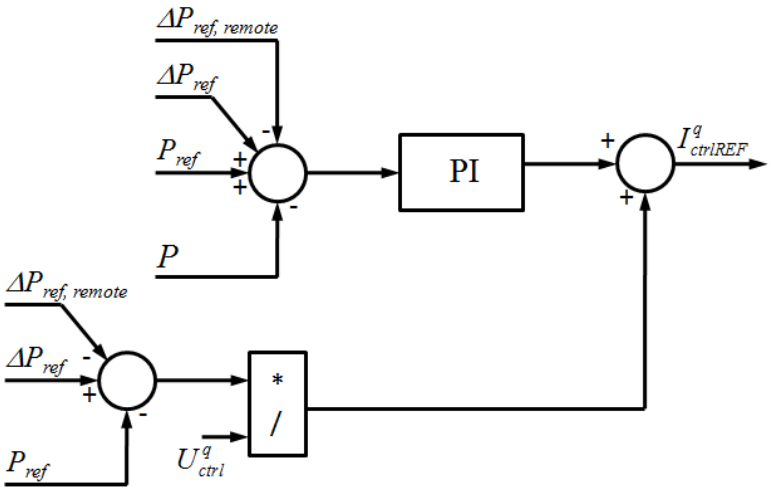

Figure 4-17 Block diagram of the frequency regulation control

In Figure 4-17, the power reference is modified by a variation of power setpoint determined locally by the frequency controller, and a variation of setpoint determined remotely in the system intended to contribute to the frequency regulation.

The controller, and the scheme as a whole, will be tested in Chapter 5 through simulations in SIMPOW.

Chapter 5

Operation in Parallel with AC grids and Simulations

In this Chapter, the proposed control strategy to regulate voltage, or, in other words, to balance the power in the DC system, is tested as will be explained next. The most critical scenarios will be simulated, which are, the outage of the DC voltage regulating converter, and the operation of a converter in its current limits.

Moreover, simulations aiming to show the performance of the frequency regulation scheme, proposed in Section 4.6 are presented. A scenario where a sudden decrease of load occurs in one system will be simulated to observe the response of the proposed scheme together with governor actions.

5.1 Test system description

The basic system used here is taken from [31]. This system is used in [31] to analyze small-signal stability in a simple two-area system. Originally, the system is as shown in Figure 5-1. In this grid, two AC systems are connected through an AC transmission system of 220 km length. System A is sending 439 MW to system B.

According to [31], one of the lines between bus 8 and 9 is suddenly disconnected. As a consequence of this, power oscillations occur, as shown in Figure 5-2.

This system is modified as shown in Figure 5-3. In these, two more AC systems, C and D, modeled as Thevenin equivalents (AC source in series with an impedance), are added.

In system A, generators 1 and 2 reduce their output power (compared to the original case from [31]). There is an excess of power of about 133 MW. This excess is transmitted to the DC grid through the converter A instead of the AC link between buses 7 and 9. With this re-dispatch, the loading of the AC link between buses 7 and 9 is reduced to 11 MW.

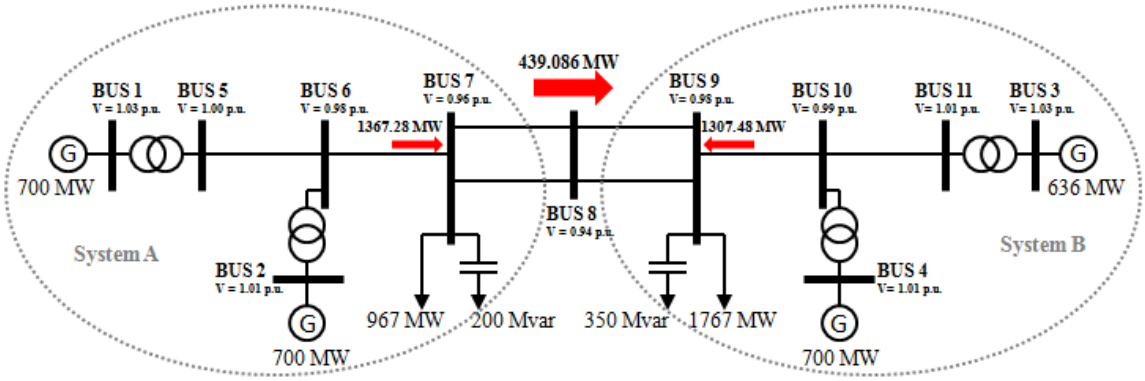

Figure 5-1 System to analyze small signal stability [31]

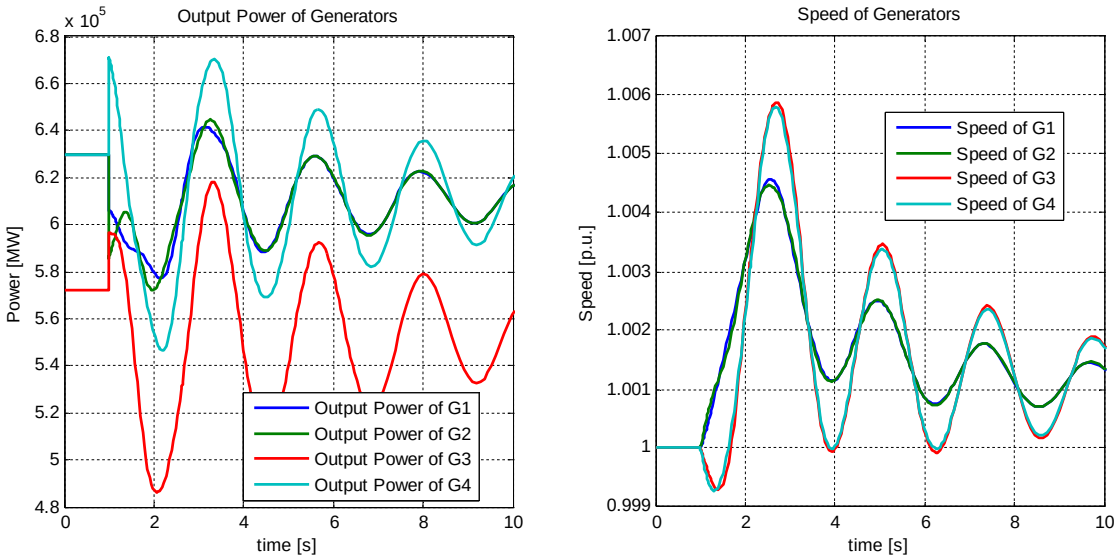

Figure 5-2 Output power and speed of generators when disconnecting line between buses 8 and 9

In system B, generator 4 generates 700 MW as originally set, while generator 3, which is the slack generator, changes its output to 714 MW (in the power flow simulation). Power from AC systems C and D, and system A are transported to system B through the converter B, which has 383 MW of output power.

System C is considered to be a “wind farm” where the converter is intended to control frequency in the AC side, so the input power (from the AC grid to the DC grid) is determined by the wind turbine power output. Since frequency control is beyond the scope of this thesis, converter C is set to control power only.

System D is another AC system with frequency regulation capability, so converter D can control either active power flow or DC voltage. These four systems (A, B, C, and D) are connected through a DC grid with a voltage level of 150 kV, as shown in Figure 5-3.

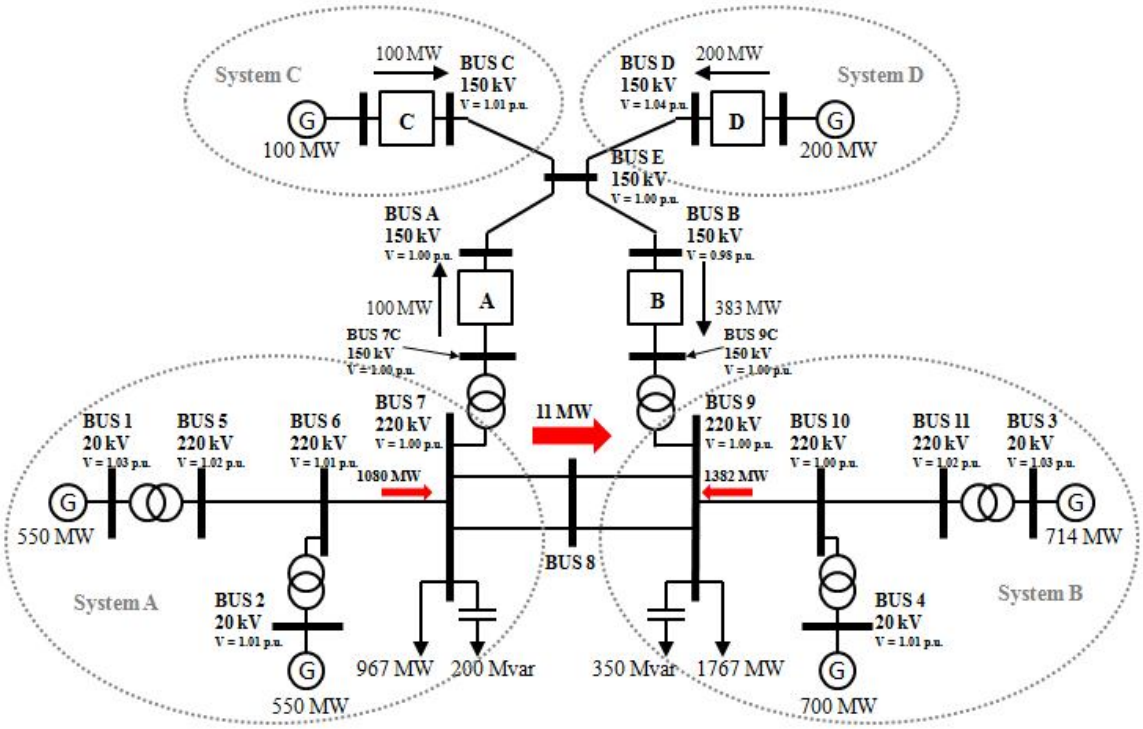

Figure 5-3 Test system of a DC grid interconnecting AC grids.

For the sake of simplicity, inductances and capacitances are neglected in the DC cables (lines) and a resistance of 0.01 Ω per kilometer is assumed. Cables between buses A and E, and B and E are assumed to have the same length as the AC link. A distance to the "wind farm" (system C) and to the AC system D are 320 and 430 km respectively. Resistances of the DC cables (lines) are listed in Table 5-1.

Table 5-1 DC cable (line) data

Line	Resistance (ohms)	Length (km)
Bus A – Bus E	1.1	110 km
Bus B – Bus E	1.1	110 km
Bus C – Bus E	3.2	320 km
Bus D – Bus E	4.3	430 km

The converter ratings are shown in Table 5-2. In this, capacitors with a time constant τ of 5 ms are selected. The switching frequency of the converters is considered to be 15 times 50 Hz, which corresponds to 4712.4 rad/s. Since the speed of the current controller should be less than the switching frequency a bandwidth of 500 rad/s is selected for all the converters.

Table 5-2 Converter ratings

Converter ID	MVA	Voltage (kV)	Capacitor (μF)	Bandwith (rad/s)
Converter A	500	150	222	500
Converter B	500	150	222	500
Converter C	300	150	133	500
Converter D	300	150	133	500

In Table 5-3 the setpoints for each converter are shown. Converters A, C, and D are selected to control the power in normal conditions, while converter B sets the DC voltage to 0.98 p.u in order to keep the voltage within 1 ± 0.05 p.u. in all nodes. Positive sign of power means that power is going into the DC grid. Negative sign would mean that power is going out the DC grid, i.e. entering the respective AC grid.

Table 5-3 Converter setpoints

Converter ID	DC voltage (p.u)	Active Power (MW)	Reactive Power (Mvar)	AC voltage (p.u.)
Converter A	---	100	0.00	---
Converter B	0.98	---	0.00	---
Converter C	---	100	---	1.00
Converter D	---	200	---	1.00

Figure 5-4 shows the results of the same simulation performed in [31], i.e. disconnecting the line between bus 8 and 9. As can be seen, since the power flow between buses 7 and 9 is reduced, power oscillations are less critical in this case.

5.2 Outage of the DC voltage regulating converter

In this simulation, the DC voltage regulating converter, i.e. converter B, is taken out of service at second 1. The intention of this simulation is to verify how the proposed control strategy accomplishes to balance the power flow in the DC grid and what the effects on the main AC system are.

As mentioned above, converter B is set to control the DC voltage, while converter C, to where the “wind farm” is connected, is set to control power. The parameters U_{DCmin} and U_{DCmax}, which correspond to the limits to enter in under/overvoltage control mode respectively, are set to 2.00 and 0.10 p.u. for converter C since it is not intended to control DC voltage by any means.

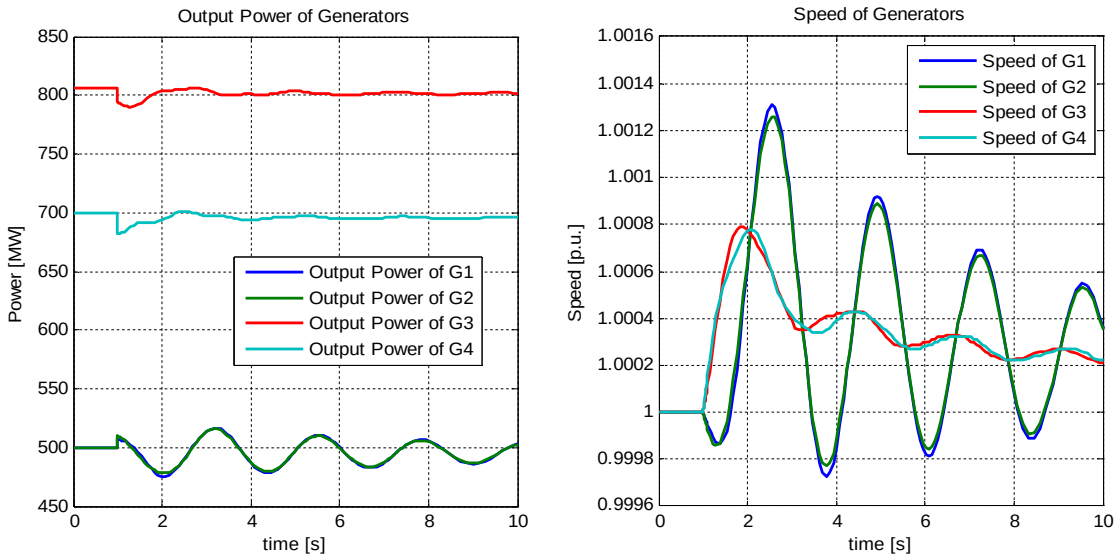

Figure 5-4 Output power and speed of generators when disconnecting line between buses 8 and 9

In the case of converters A and D, parameters U_{DCmin} and U_{DCmax} are set to 0.95 and 1.05 p.u. respectively. It means that the converters will control a constant power unless the voltage is out of this range. If not, converters will go into under/overvoltage control mode. As explained in Section 2.5.4, a wider range of admissible voltages is needed, that is, if an event occurs that results in any of the converters to go to under/overvoltage control mode, the DC voltage should be allowed to reach 0.9/1.1 p.u. respectively. So according to this, the factor *k* can be calculated as follow (base voltage 150 kV and MVA base 100 MVA):

For converters A and B

$$k = (1.10 - 1.05)/(2\times5) = 0.00500 \tag{5.1}$$

For converters *C* and *D*

$$k = (1.10 - 1.05)/(2\times3) = 0.00833 \tag{5.2}$$

In Table 5-4 the parameters for the power – voltage curves are listed.

Table 5-4 Parameters of the converter power – voltage control (Section 2.5.4)

Converter ID	U_{DCmax} (p.u.)	U_{DCmin} (p.u.)	P_{ref} (p.u.)	k (p.u)
Converter A	1.05	0.95	1.00	0.00500
Converter B	---	---	---	---

Converter C	2.00	0.10	1.00	0.00500
Converter D	1.05	0.95	2.00	0.00833

Figure 5-5 shows the simulation results. It can be seen that, at second 1, converter B's output power suddenly goes to zero, which means that it is out of service. DC voltage starts increasing since input power is higher than output power. Converter A enters to its overvoltage control mode, and decreases its input power even changing its direction. Input power of converter C remains unchanged, as desired. Converter D enters to its overvoltage control mode, and decreases its output to almost zero. Then, the exchange of power among the AC systems is mainly 100 MW from system C to the main system (A and B).

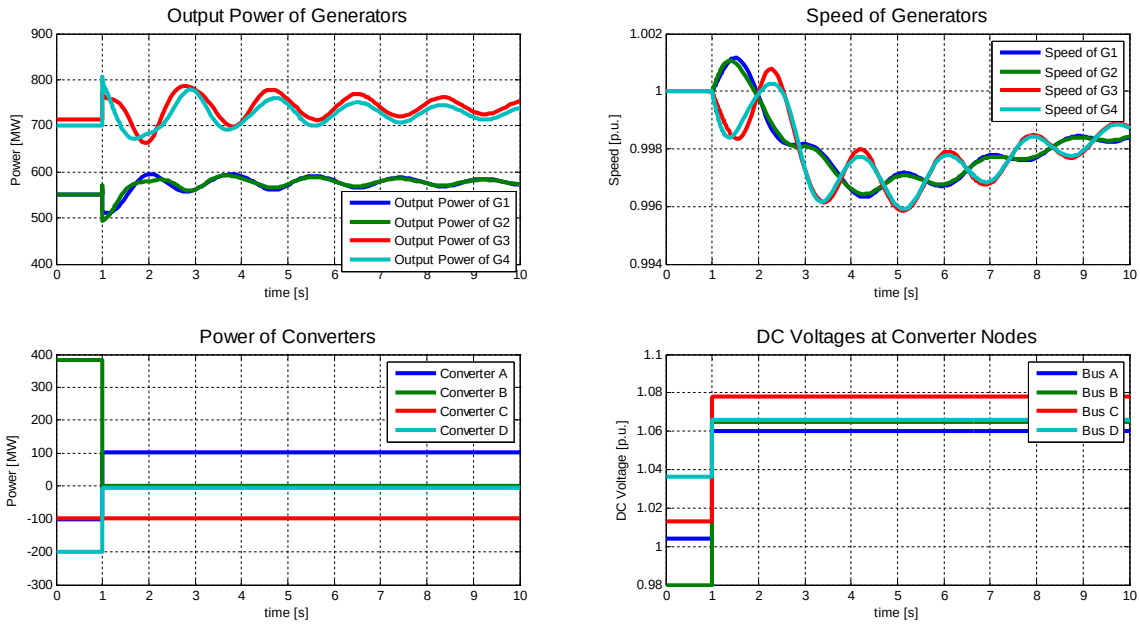

Figure 5-5 Simulation results when converter A is suddenly disconnected.

As a consequence of the converter outage, a sudden redistribution of the power flow occurs in the main AC system (A plus B), resulting in power oscillations. However, these power oscillations are not observed in the DC grid, which means that power oscillation in one system is not spread to the other systems.

5.3 Converter reaching its current limit

The aim of this simulation is to observe the behavior of the DC system when one of the converters has reached its current limit. DC voltage regulating converter is more likely to reach the current limit since it is in charge of balancing the power flow in the DC grid.

For this case, the power setpoints are re-scheduled as shown in Figure 5-6. In total, 570 MW is imported to the main system (A plus B) through converters A and B. Converter A

is set to control the DC voltage, to 0.98 p.u. This value is chosen in order to keep voltage in the DC grid at all DC nodes within ± 5 % the rated voltage.

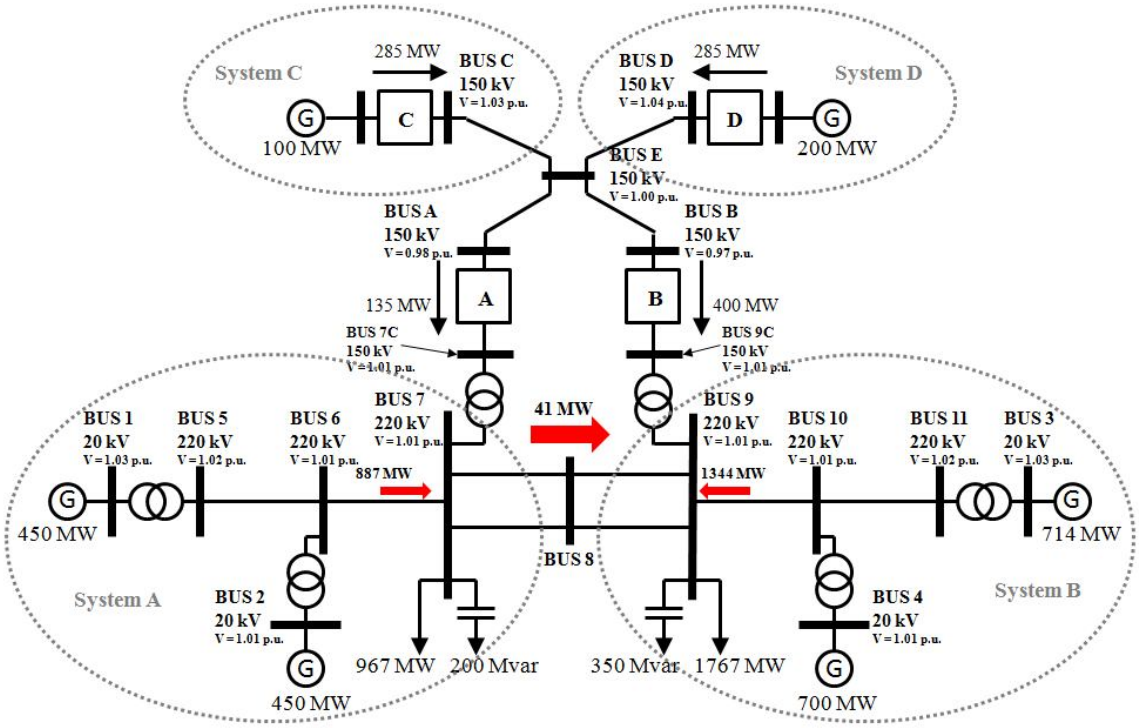

Figure 5-6 Test system of a DC grid interconnecting AC grids.

The simulated event is the disconnection of the converter B, so that the converter A, which is regulating the DC voltage, will have to transport the power from systems C and D, to the main system. However, the rated power of the converter is 500 MVA, which gives a current limit of 5 p.u. (Base voltage 150 kV, base power 100 MVA). When the converter reaches 5 p.u. the converter A will stop regulating DC voltage and will set a constant current as established in Section 4.2.

The results are shown in Figure 5-7. The parameters of the under and overvoltage control mode are the same than the ones shown in Table 5-4.

It can be seen in Figure 5-7 that when converter B is disconnected, converter A tries to balance the power in the DC grid compensating the loss of output power from converter B. However, as can be seen in the Figure 5-8, converter A reaches its current limit and can no longer control the DC voltage. Input power of converter C remains unchanged as desired.

The DC voltage increases, and reaches U_{DCmax} at converter D going, then, into its overvoltage control mode. Due to this, converter D changes its ouput power according to its power-voltage curve. The DC system, finally, is balanced.

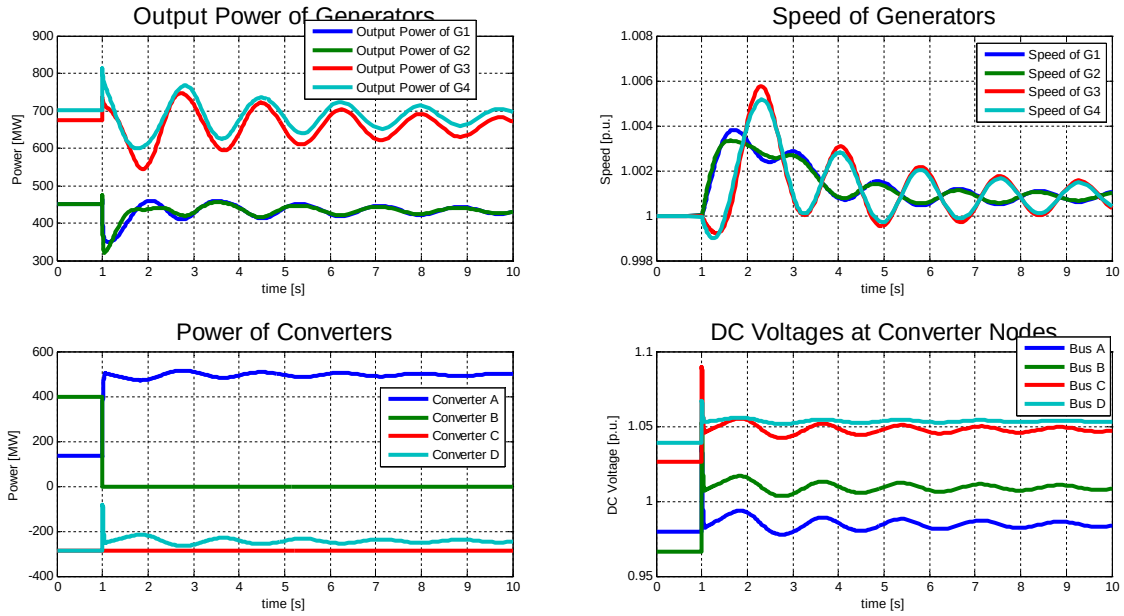

Figure 5-7 Simulation results when converter A reaches its current limit.

However, oscillations are observed in the DC grid. This can be explained looking at the Figure 5-8. It can be seen that converter A stops regulating the DC voltage and reaches its limit which is 5 p.u. Due to disconnection event, power oscillations appear in the AC side, which causes the AC voltages to oscillate as well. Due to oscillating voltage and the fixed current, the resulting power is also oscillating, and this is transferred to the DC grid. These power oscillations are transferred to the converter D, which transfer these oscillations to its AC system.

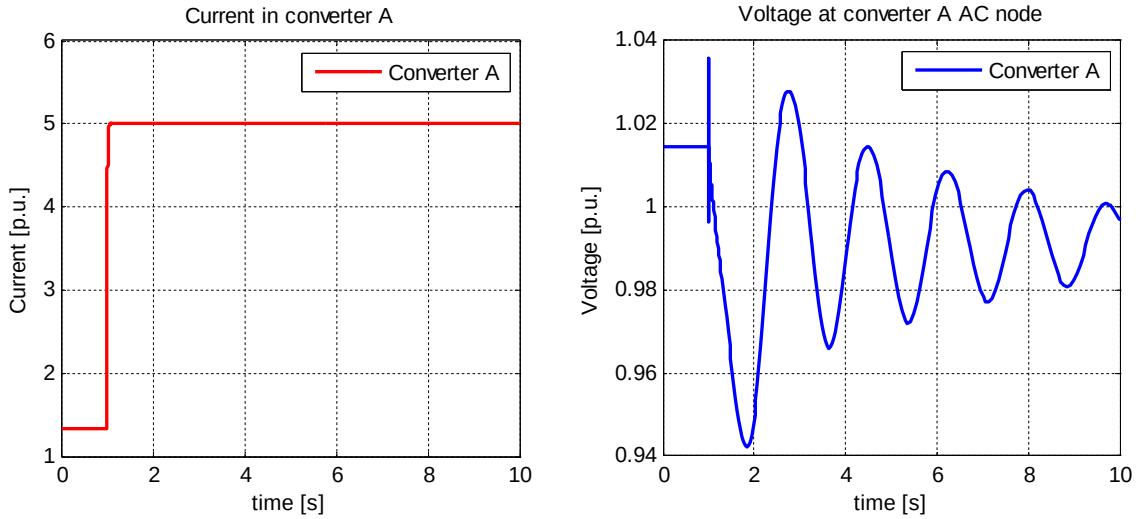

Figure 5-8 Current and voltage in the AC side of the converter A.

5.4 Frequency regulation controller

A scheme to regulate frequency among separated AC systems, but connected through a DC grid is proposed in Section 4.6 and will be tested in this Section. The test system will be equal to the one used in Section 5.3, with the difference that a 4 000 MVA generator is connected instead of an ideal AC source. The same governor and exciter used for generators at systems A and B are used but with the corresponding ratings.

The simulated event is a disconnection of 15 % of the load connected at the bus 9, which is 265 MW of power. With this event, the system response will be analyzed for three different cases as shown next.

5.4.1 Without Frequency Regulation Controller in Operation

The event mentioned above is simulated with no frequency regulation controller in operation at any converter. The results are shown in Figure 5-8.

It can be seen that the steady state frequency in the AC system after the disconnection event is 50.15 Hz (1.003 × 50), and the output power from generators has decreased. Input/output power of converters and DC voltages remain constant. This means that systems C and D are not affected by the event occurred in the main system.

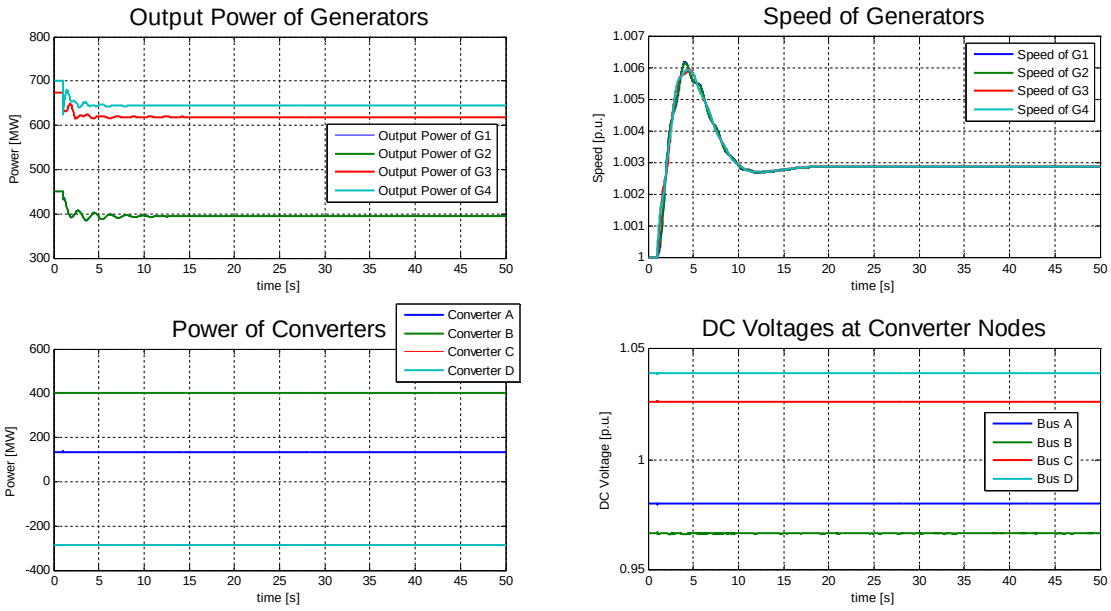

Figure 5-8 Simulation results when there is a disconnection of 265 MW with frequency regulation control deactivated

5.4.2 With Frequency Regulation in Operation at Converter B

In the following simulation, the frequency regulation control at converter B is activated and coordinated with converter D, so that the change on power setpoint at converter B is sent to converter D. Frequency regulation control at converter D is not activated. The required parameters are the percent of frequency regulation R, and the time constant T_G. In converter B, R will be calculated as follows:

$$R_B = \frac{0.1/50}{500/100} = 0.0004 \tag{5.3}$$

And for converter D:

$$R_D = \frac{0.1/50}{300/100} = 0.00067 \tag{5.4}$$

Where R_B and R_D are in p.u (Base frequency 50 Hz, power MVA 100 MVA). The effects of the time constant T_G will be analyzed with simulations for different values of T_G. T_G will determine the speed of the frequency regulation controller.

Figure 5-9 shows frequency curves for different values of T_G. From them, a time constant of T_G of 30 s will be selected.

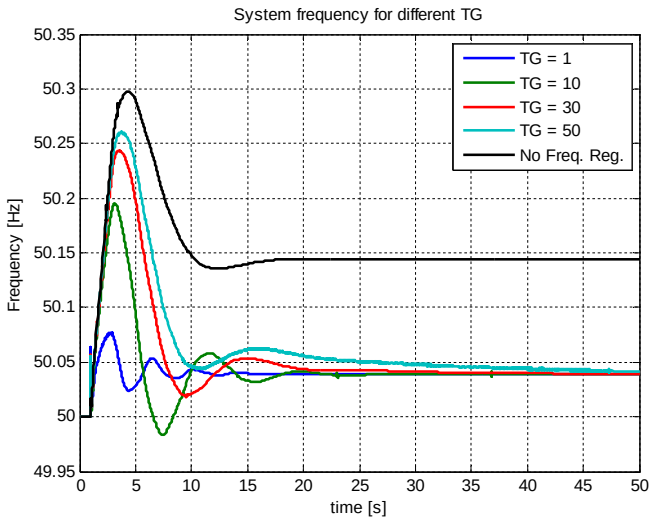

Figure 5-9 Frequency at converter B terminal for different T_G

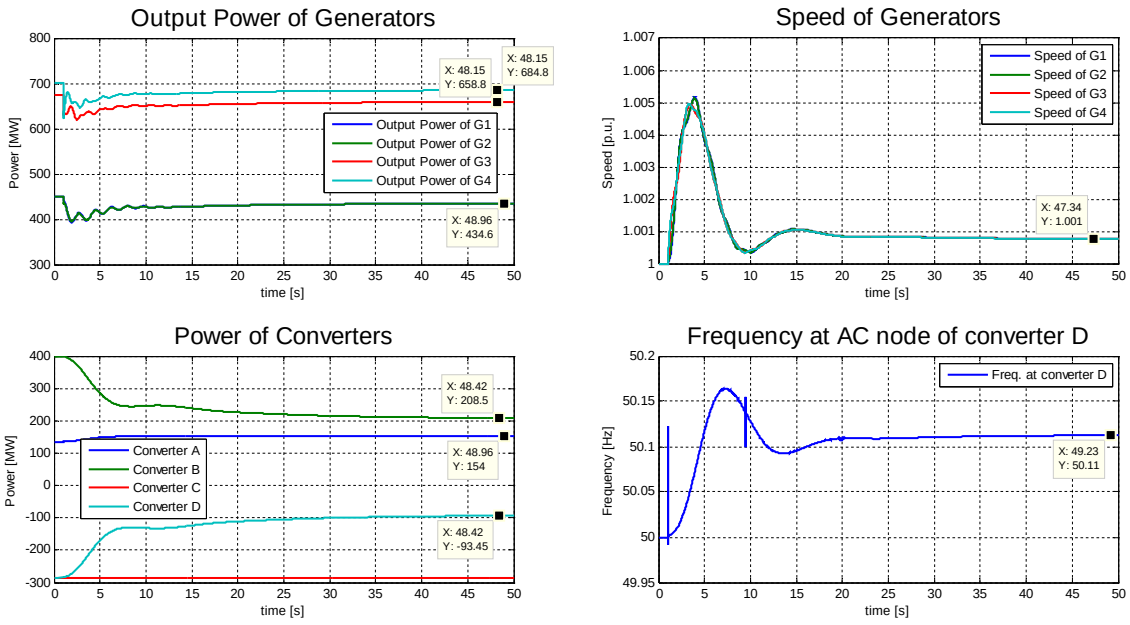

Figure 5-10 Simulation results when there is a disconnection of 265 MW with frequency regulation control activated at converter B

Figure 5-10 shows that frequency in the main system has improved when the frequency regulation controller in converter B is activated. The frequency in the main system is now 1.001 × 50 Hz which is 50.05. However, it affects the frequency at system D where, it is increased to 50.11 Hz, almost the same value than the main system in the previous case, where no frequency regulation controller has been activated. So, the problem has been transferred from the main system to system D.

It is interesting to observe the change of power from pre-event to post-event time. In Table 5-5 it is summarized these changes.

Table 5-5 Comparison of power between pre and post event conditions.

Element	Pre-event (MW)	Post-event (MW)	Difference (MW)
Generator 1	450	435	-15
Generator 2	450	435	-15
Generator 3	714	659	-55
Generator 4	700	685	-15
Converter A	135	154	19
Converter B	400	209	-191
Converter C	-285	-285	0
Converter D	-285	-93	192

It can be seen that the main contribution for the frequency regulation has come from the output power reduction of the converter B, being almost 72 % of the total of load lost in the event. This is due to the R factor chosen, since R_B equal to 0.1 Hz / 500 MW means that the converter will contribute with 500 MW (either reduction or increase) if a change of 0.1 Hz occurs. The selection of R must be according to the criteria of the system operator.

For the following simulations, the values calculated in (5.3) and (5.4) will be kept.

5.4.3 With Frequency Regulation in Operation at Converter B and D

Now, both converters, B and D, are allowed to help AC system to regulate power. In this case, converter D also will respond to the change of frequency in its system.

Figure 5-11 shows the results of the simulation when both frequency regulation controllers, at converter B and D, are used. As explained in Section 4.6, both controllers will send each other its respective variation of power setpoint as a function of the change in frequency.

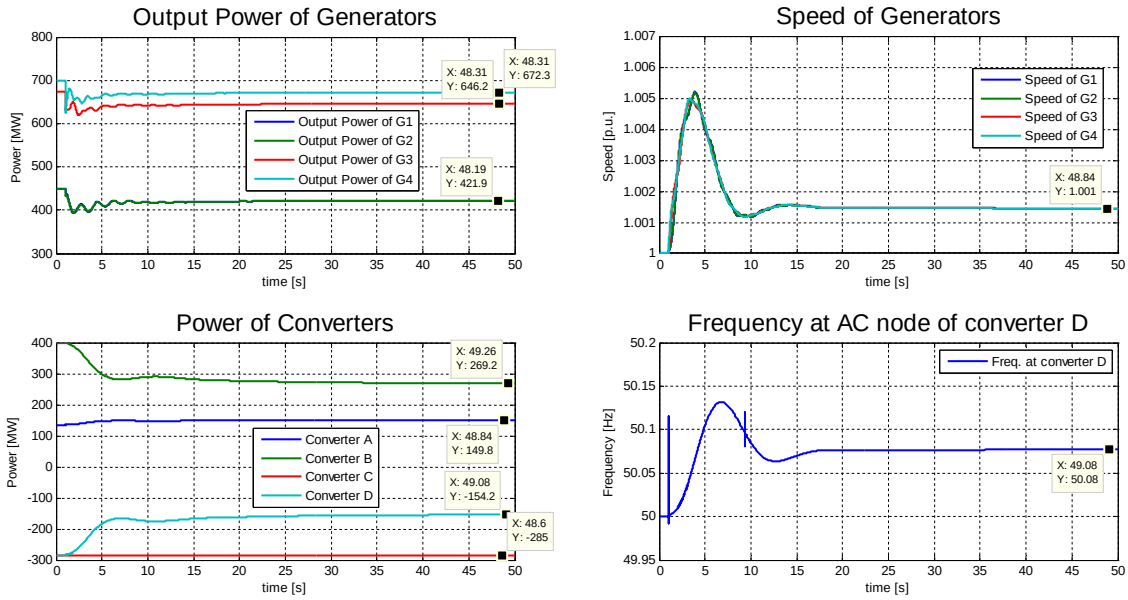

Figure 5-11 Simulation results when there is a disconnection of 265 MW with frequency regulation control activated at converter B and D

From Figure 5-11, it can be seen that frequency in the main system is now, 1.00145 × 50 = 50.0725 Hz (zooming the Figure) and in system D it is 50.08 Hz. If we take into consideration [16] where it is claimed that allowable deviation limit of frequency is ± 0.1 Hz in Nordel, then, the frequency obtained when both frequency regulating controllers (B and D) could be considered as acceptable.

In table 5-6 it is shown a comparison of the frequency in every simulation.

Table 5-6 Comparison of power between pre and post event conditions.

Case	Main System (Hz)	System D (Hz)
1. With no Freq. Reg.	50.15	50.00
2. With Freq. Reg. at Conv. B	50.05	50.11
3. With Freq. Reg. at Conv. B & D	50.07	50.08

If a maximum deviation of ± 0.1 Hz is considered acceptable, then case 1 is not acceptable for the main system and it is excellent for system D. Case 2 is excellent for system B while it is not acceptable for system D. Finally, case 3 is acceptable for both of them, although a perturbation has been transferred to a system not involved in the perturbation.

Table 5-7 shows a comparison between the pre post-event powers. As can be seen, the contribution from the converters has decreased, as compared to the previous case (Table 5-5) leading to a cooperation that satisfies the requirements of frequency regulation, even if both systems are not synchronously connected.

Table 5-7 Comparison of power between pre and post event conditions.

Element	Pre-event (MW)	Post-event (MW)	Difference (MW)
Generator 1	450	422	-28
Generator 2	450	422	-28
Generator 3	714	646	-68
Generator 4	700	672	-28
Converter A	135	150	15
Converter B	400	269	-131
Converter C	-285	-285	0
Converter D	-285	-154	131

Chapter 6

Conclusions and Future Work

6.1 Summary and conclusions

In this thesis, the operation of a DC grid has been investigated with focus in the power balance in the DC grid and frequency regulation between separate AC systems but connected through a DC grid. In this thesis, three stages of work can be noticed. First, a brief review of proposed control strategies in the literature has been carried out with the aim of understanding the problem of power flow balancing in the DC grid. Second, the modeling of VSC-HVDC and its respective controller has been implemented together with the proposed control strategy and the frequency regulation scheme. Finally, simulations to test the proposed control strategy for the DC system together with an AC system have been performed.

It has been found that the capacitors play an important role in the dynamics performance of the DC grid. Since capacitor dynamics are in the order of milliseconds, fast action must be taken when facing a contingency. To rely in manual actions or mechanical switching could be of little help due to the speed of the DC grid dynamic. Since the controllers of VSC are usually fast, automatic actions coming from them are suitable to accomplish the power balance in the DC grid when a contingency occurs.

A control strategy that uses the DC voltage as in indicator of power balance is used. This control strategy, based on [14], [18], and [19], emulates the primary frequency control of AC systems. When the DC voltage goes up, it means that there is excess of input power, initiating then, the reduction of input power, similar to overfrequency generator disconnections. Thanks to the flexibility of VSC, output power, which would correspond to load in AC systems, will be increased to meet the excess of input power in the DC grid. Analogously, when DC voltage goes down, which means deficit of input power, it will initiate the reduction of output power, similar to the underfrequency load shedding schemes of AC systems.

A simple frequency regulation scheme has been implemented. It emulates the proportional controller of machines governors. In this scheme, the variation of frequency measured at the converter node is used as input, getting as output the variation of power

setpoint. This variation of power setpoint will be sent to the selected converter that will contribute with control the frequency regulation task, so a communication channel is required for this scheme to work.

Simulations shows that the proposed control strategy to the DC regulate voltage works properly, and that, after a severe contingency (like the loss of the DC voltage regulating converter), the power setpoints are re-arranged so that the system reaches a new steady state operation point automatically. However, it must be bear in mind that the converter and the controller model are simplified and the proposed control strategy should be further investigated with detailed models. Another interesting result from the simulations is that, as long as converters don't reach their current limit, power oscillation in one AC system doesn't affect the performance of the DC grid at all. This is because converters are fast enough to react properly to power oscillations. However, when one converter reaches the current limit, oscillations can be transferred from one AC system to another.

Frequency regulation also was tested with simulations, and frequency variations could be effectively mitigated. In the simulations three cases were simulated and it was found that the best scenario, for systems that cooperate in the frequency regulations, was when in both, the frequency regulation control is turned on.

6.2 Future Work

In this thesis one simplified model of VSC together with its controller has been implemented in SIMPOW, but neglecting electromagnetic transients in AC side. Due to this, phasors calculations can be used and the simulation time is decreased considerably, being suitable for power system studies. In order to carry out exhaustive system studies, this model should be contrasted with a detailed model implemented in an ETM program. The validity of the model for faults can be investigated as well, and its further extension for unsymmetrical events can be a future task regarding the modeling part.

In Section 2.5 some questions regarding the operation of a DC grid were stated. In this thesis, only two of those questions were partially answered, they are:

After a contingency, if voltage-regulating converters reach their limits, how to allocate the balancing task to the other converters?

In order to solve this issue, a control strategy that aims to regulate the DC voltage after a converter outage was proposed.

In case of deficit of input power, how should inverters behave?

This question was answered proposing the undervoltage control mode, where, in the case of the inverter, it would reduced its output power, similar to the underfrequency load shedding of AC systems.

However, criteria to determine the parameters of the power – voltage curves are not discussed in this thesis. Also the location of converters that will control the DC voltage, in certain contingencies, is not investigated. Regardless the control strategy used in the future HVDC grids, these issues would demand exhaustive system studies to allocate the DC voltage regulating converters and to designate optimal setpoints that will work for normal conditions and for N-1 contingencies as well.

Another issue mentioned in this thesis was the preventions of overload of the DC cables or lines. In a DC grid the power flow over the cables (lines) will be distributed according to their resistances, or, in other words, power flow over cables is not controlled. Prevention of overload in cables must also be investigated.

About frequency regulation, the time response of the frequency regulation control proposed should be further investigated, since in the simulation, a fast response introduced frequency oscillations of low amplitude, while a slow response gives a similar response to the machine dynamics. Events like power oscillations, that don’t involve, necessarily, power unbalances, but imply frequency oscillations, may affect the performance of the frequency regulation scheme and it should be further investigated.

References

[1] Robert Rudervall, J.P. Charpentier, Raghuveer Sharma, “High Voltage Direct Current (HVDC) Transmission Systems Technology Review Paper,” in *Energy Week 2000*, Washington, D.C, USA, March 2000.

[2] ABB, “The early HVDC development,” available from: http://www05.abb.com/global/scot/scot221.nsf/veritydisplay/8cf1c44dbc522685c12574e9006051a5/$File/The%20early%20HVDC%20development.pdf

[3] EWEA, “Oceans of Opportunity,” Available from: http://www.ewea.org/fileadmin/ewea_documents/documents/publications/reports/Offshore_Report_2009.pdf, September 2009.

[4] K. Eriksson, P. Halvarsson, D. Wensky, M. Häusler, “System Approach on Designing an Offshore Wind Power Grid Connection,” Available from: http://library.abb.com/global/scot/scot221.nsf/veritydisplay/34ec041beda66334c1256fda004c8cc0/$File/03MC0132%20Rev.%2000.PDF

[5] German Aerospace Center, Institute of Technical Thermodynamics, Section System Analysis and Technology Assessment, “Trans-Mediterranean Interconnection for Concentrating Solar Power,” Available from: http://www.dlr.de/tt/trans-csp

[6] J. Reeve, “Multiterminal HVDC Power Systems”, *IEEE Transaction on Apparatus and Systems*, Vol. PAS-99 No. 2, March/April 1980.

[7] W. F. McNichol, J. Reeve, J. R. McNichol, R. E. Harrison, J. P. Bowles, “Considerations for Implementing Multiterminal DC Systems,” *IEEE Transaction on Power Apparatus and Systems*, Vol PAS-104, September 1985.

[8] Victor F. Lescale, Abhay Kumar, Lars-Erik Juhlin, Hans Björkmlund, Krister Nyberg, “Challenges with Multi-Terminal UHVDC Transmissions,” *POWERCON 2008 IEEE India Conference*, October 12-15, New Delhi, India, 2008.

[9] K.W. Kanngiesser, E. Rumpf, J.P. Bowles, J. Reeve, A. Ekstrom, "HVDC Multiterminal Systems," *Cigré*, 14-08, 1974 (Electra.), August, 1974.

[10] Lianxiang Tang, and Boon-Teck Ooi, "Locating and Isolating DC Faults in Multi-terminal DC Systems," *IEEE Transaction Delivery*, Vol. 22, No 3, July, 2007.

[11] Adelina Agap, Cristina Madalina Dragan, "Multiterminal DC Connection for Offshore Wind Farms," Master Thesis, Aalborg University, Denmark, 2009.

[12] W. F. Long, J. Reeve, J. R. McNichol, M. S. Holland, J. P. Taisne, J. LeMay, D. J. Lorden, "Application Aspects of Multiterminal DC Power Transmission," *IEEE Transaction on Power Delivery*, Vol. 5, No 4, November, 1990.

[13] ABB, "The Québec – New England Transmission," available from: http://www.abb.com/cawp/gad02181/ca531f1f7141cb8bc125766a0045817c.aspx

[14] Tatsuhito Nakajima, Shoichi Irokawa, "A Control System for HVDC Transmission by Voltage Source Converters," *IEEE Power Engineering Society Summer Meeting*, 1999.

[15] Cuiqing Du, "VSC-HVDC for Industrial Power Systems," Phd Thesis, Department of Energy and Environment, Chalmers University of Technology, Göteborg, Sweden, 2007.

[16] Tuan A. Le, "Lecture notes on Frequency Control: An Overview, for the course of Power System Operation," Department of Energy and Environment, Chalmers University of Technology, Göteborg, Sweden, February, 2009.

[17] B. K. Johnson, R. H. Lasseter, F. L. Alvarado, R. Adapa, "Expandable Multiterminal DC Systems Based on Voltage Droop," *IEEE Transactions on Power Delivery*, Vol. 8, No. 4, October, 1993.

[18] Temesgen M. Hailesalassie, Marta Molinas, Tore Undeland, "Multi-terminal VSC-HVDC System for Integration of Offshore Wind Farms and Green Electrification of Platforms in the North Sea," *NORPIE 2008*, Espoo, Finland, 9 - 11 June, 2008.

[19] Temesgen Haileselassie, Kjetil Uhlen, Tore Undeland, "Control of Multiterminal HVDC Transmission for Offshore Wind Energy," *Nordic Wind Power Conference*, 10 - 11.09.2009, Bornholm, Denmark.

[20] Lie Xu, W. Williams, Liangzhong Yao, "Multi-terminal DC Transmission Systems for Connecting Large Offshore Wind Farms," *Power and Energy Society General Meeting – Conversion and Delivery of Electrical Energy in the 21st Century*, 2008 IEEE, 20-24 July, 2008.

[21] J. Arrillaga, C. P. Arnold, "Computer Analysis of Power Systems," *University of Canterbury*, *John Wiley & Sons*, 1990.

[22] STRI AB, "SIMPOW User Manual 11.0," Release 11, Sweden, 2010.

[23] Ned Mohan, Tore M. Undeland, William P. Robbins, "Power Electronics Converters, Applications and Design," Third Edition, John Wiley & Sons, Inc, USA, 2003.

[24] Stijn Cole, Jef Beerten, Ronnie Belmans, "Generalized Dynamic VSC MTDC Model for Power System Stability Studies," *IEEE Transactions on Power Systems*, Vol 24, No. 4, November, 2009.

[25] Massimo Bongiorno, "Lecture notes on Tools and Transformation for the course Power Electronic Solutions for Power Systems," Department of Energy and Environment, Chalmers University of Technology, Göteborg, Sweden, October, 2009.

[26] Massimo Bongiorno, "Course Material: Transformation for Three Phase Systems," Department of Energy and Environment, Chalmers University of Technology, Göteborg, Sweden, October, 2009.

[27] Fainan Hassan, Math Bollen, "Dynamic current limitation to provide interactive features of power-electronics interfaced distributed generation," *Electrical Power Quality and Utilization Magazine*, Vol.3, No.2, October, 2008.

[28] It´s time to connect – Technical description of HVDC Light®technology. Available from : http://www.abb.com.hvdc, 2009-06-25.

[29] Lena Max, "Design and Control of a DC Collection Grid for a Wind Farm," Phd. Thesis, Department of Energy and Environment, Chalmers University of Technology, Göteborg, Sweden, 2009.

[30] Per Karlsson, "DC Bus Voltage Control for a Distributed Power System" Phd Thesis, Department of Industrial Electrical Engineering and Automation, Lund, University, Lund, Sweden, 2002.

[31] P. Kundur, "Power System Stability and Control," McGraw-Hill, USA, 1994.